RSC Advances

PAPER

View Article Online
View Journal | View Issue

Cite this: *RSC Adv.*, 2019, **9**, 15470

Silver derivatives of multi-donor heterocyclic thioamides as antimicrobial/anticancer agents: unusual bio-activity against methicillin resistant *S. aureus*, *S. epidermidis*, and *E. faecalis* and human bone cancer *MG63* cell line†

Jaspreet K. Aulakh,[a] Tarlok S. Lobana,[*a] Henna Sood,[b] Daljit S. Arora,[b] Raminderjit Kaur,[c] Jatinder Singh,[c] Isabel Garcia-Santos,[d] Manpreet Kaur[e] and Jerry P. Jasinski[e]

The basic aim of this study pertains to the synthesis of silver nitrate complexes and the study of their antimicrobial and anticancer bio-activity. A series of new silver(I) derivatives of *N*-substituted-imidazolidine-2-thiones (L-NR, R = Et, Pr^n, Bu^n, Ph), purine-6-thione ($purSH_2$), 2-thiouracil ($tucH_2$), pyrimidine-2-thione (pymSH) and pyridine-2-thione (pySH) of composition $[Ag(S\text{-}L\text{-}NR)(PPh_3)_2(ONO_2)]$ {R = Et (**1**), Pr^n (**2**), Bu^n (**3**), Ph (**4**)}, $[Ag_2(N,S\text{-}purSH_2)_2(\mu\text{-}dppm)_2](NO_3)_2\cdot 2H_2O$ (**5**) (dppm = $Ph_2P{-}CH_2{-}PPh_2$), $[Ag(L)(PPh_3)_2](NO_3)$ {L = N,S-$purSH_2$ (**6**); S-$tucH_2$ (**7**)}, $[Ag(N,S\text{-}pymS)(PPh_3)_2](CH_3OH)$ (**8**), and $[Ag(N,S\text{-}pyS)(PPh_3)_2]$ (**9**) have been synthesized and structurally characterized. These new and some previously reported complexes {$[Ag_2(L\text{-}NH)_4(PPh_3)_2](NO_3)_2$ (**10**), $[Ag(L\text{-}NMe)_2(PPh_3)](NO_3)$ (**11**), and $[Ag(S\text{-}bzimSH)_2(PPh_3)_2](OAc)$ (**12**), L-NH = 1,3-imidazolidine-2-thione; L-NMe = 1-methyl-3-imidazolidine-2-thione and $bzimSH_2$ = benzimidazoline-2-thione)} have shown moderate to high anti-microbial activity against Gram positive bacteria, namely methicillin resistant *Staphylococcus aureus* (MRSA) and *Staphylococcus aureus* (MTCC 740), and Gram negative bacteria, namely *Staphylococcus epidermidis* (MTCC 435), *Enterococcus faecalis* (MTCC 439), *Shigella flexneri* (MTCC 1457) and a yeast *Candida albicans* (MTCC 22). These complexes have also been found to be bio-safe as studied using MTT [3-(4,5-dimethylthiazol-2-yl)-2,5-diphenyl tetrazolium bromide] assay. The anti-tumor study of silver complexes against human osteosarcoma cell line (MG63) has shown IC_{50} values in the range of 6–33 μM.

Received 9th March 2019
Accepted 15th April 2019

DOI: 10.1039/c9ra01804b

rsc.li/rsc-advances

Introduction

Silver is an important metal known since ancient times for its antiseptic and antibacterial properties. Silver compounds are used to control bacterial growth in a variety of medical applications.[1,2] For example, silver nitrate was introduced in therapeutic applications in 1884 for the prevention of ophthalmia neonatorum,[3] and in eye drops against eye infections.[1,2,4] Further, silver(I) sulfadiazine is used to treat severe burns to protect them from bacterial infection and catalyzes skin renewal,[5] while a silver sulfadiazine–chlorhexidine mixture is used against catheter infections *in vivo*.[6,7] Silver is even present in the human body (absorbed through the lungs, gastrointestinal tract, mucus membranes and skin) and any excess amount is eliminated from the body through the urine and faeces.[2,8] Polymeric silver compounds of ethanediyl bis(isonicotinate) have also been used in coatings of implant materials for killing bacterial infections while remaining biocompatible for cell growth.[2,9] In view of the above uses, the investigation of silver(I) chemistry becomes exceptionally appealing, which is bolstered by the ability of this metal to form complexes of variable geometry and nuclearity.[10–16] Literature reports reveal that silver(I) complexes of sulfur containing ligands have found application in medicines, analytical chemistry and polymer industry.[10–12,17,18]

In the literature, coordination chemistry of silver(I) with several heterocyclic-2-thiones, namely imidazolidine-2-thiones (L-NH, L-NMe), imidazoline-2-thiones, *N*-methylbenzothiazole-2-thione, pyrimidine-2-thione, tetrahydropyrimidine-2-thione,

[a]*Department of Chemistry, Guru Nanak Dev University, Amritsar-143 005, India. E-mail: tarlokslobana@yahoo.co.in; Fax: +91-183-2258820*

[b]*Department of Microbiology, Guru Nanak Dev University, Amritsar-143 005, India*

[c]*Department of Molecular Biology and Biochemistry, Guru Nanak Dev University, Amritsar-143 005, India*

[d]*Departamento de Quimica Inorganica, Facultad de Farmacia, Universidad de Santiago, 15782-Santiago, Spain*

[e]*Department of Chemistry, Keene State College, Keene, NH 03435-2001, USA*

† Electronic supplementary information (ESI) available: Detailed IR spectra, $^1H/^{13}C$-NMR spectra, and ESI-MS isotopic patterns. CCDC 1878467, 1878471, 1878472, 1878468, 1878469 and 1878470. For ESI and crystallographic data in CIF or other electronic format see DOI: 10.1039/c9ra01804b

pyridine-2-thione, benzoxazoline-2-thione, thiazolidine-2-thione, and benz-imidazoline-2-thione, using different anions (NO_3^-, ClO_4^-, $F_3CSO_3^-$, NCS^-, SO_4^{2-}, BF_4^-) as well as halides has been reported.[13–44] Among them several silver complexes have found use as anti-microbial,[23,30,35,37,40–42] anti-tumor,[17,18,36,38,39] anti-inflammatory[18,23] and anti-malarial agents.[39] In regard to the antimicrobial activity, complexes of silver(I) salts with the thio-ligands, namely, imidazolidine-2-thione,[30,40] thiazolidine-2-thione,[41] benzo-thiazoline-2-thione,[41] *N*-methyl-imidazoline-2-thione,[42] pyrimidine-2-thiones,[23] 4,6-diamino-5-hydroxypyrimidine-2-thione,[35] pyridine-2-thione,[30] diazinane-2-thione,[30] and 2-mercapto-nicotinic acid[37] have shown activity against *Escherichia coli*,[23,30,37,40] *Pseudomonas aeruginosa*,[30,35,40] *Bacillus subtilis*,[23,37] *Bacillus cereus*,[23] *Staphylococcus aureus*,[23,35,37] *Pseudomonas aeruginosa*,[37] molds {*Aspergillus niger*,[35,37] *Penicillium citrinum*,[30,35,37], *Rhizopus stolonifer*,[37] *Aureobasidium pullulans*,[37] *Fusarium moniliforme*,[34] *Cladosporium sphaerospermum*[34]} and yeasts {*Candida albicans*,[26,32,34] and *Saccharomyces cerevisiae*[30]}. It is pointed out here that the investigations merely report antimicrobial activity without any mention of their biosafety.[23,30,35,37,39,41,42] The anti-cancer/tumor activity of complexes of silver(I) with pyrimidine-2-thiones,[36] tetrahydropyrimidine-2-thione,[17] pyridine-2-thiones,[36] thiazolidine-2-thione,[39] 5-chloro-2-mercaptobenzothiazole,[18] and 2-mercaptonicotinic acid,[18] pertains to *in vitro* cytotoxic activity against murine leukemia (L1210),[17,36] human T-lymphocyte (Molt4/C8 and CEM) cells,[17,36] breast cancer cell lines (MDA-MB-231, MCF-7),[39] colon cancer cell line (HT-29),[39] leiomyosarcoma cancer cells (LMS),[18] and breast cancer cell line (MDA-MB-231),[38] some of which have shown activity even higher than that of the anti-cancer drug cisplatin.

From our laboratory, coordination chemistry of coinage metals (Cu, Ag) with heterocyclic-2-thiones has been investigated which showed interesting chemical activity such as rupture of C–S bond[45–49] and formation of a variety of coordination complexes.[50–57] As a part of our interest to pursue bioactivity of metal-heterocyclic-2-thione complexes, we recently reported synthesis and antimicrobial activity of several copper(I)/silver(I) halide complexes of imidazolidine-2-thiones (L-NR, R = H, Me, Et, Pr^n, Bu^n, Ph) with or without triphenylphosphine (PPh_3) as a co-ligand.[44,58,59] These complexes showed moderate to high activity against various bacteria, *Staphylococcus aureus*, methicillin resistant *Staphylococcus aureus* (MRSA), *Staphylococcus epidermidis*, *Enterococcus faecalis*, *Klebsiella pneumoniae*, *Salmonella typhimurium*, *Shigella flexneri*, *Escherichia coli*, *Candida albicans* and *Candida tropicalis*, but only a few of them were biosafe.[44,58,59]

Keeping in view the high profile medicinal activity of silver(I) compounds with nitrate as anion as well as in continuation of our interest in this area,[44,58,59] in this investigation, a series of silver derivatives of thio-ligands, *N*-substituted-imidazoldine-2-thiones, (L-NR, R = Et, Pr^n, Bu^n, Ph), purine-6-thione ($purSH_2$), 2-thiouracil ($tucH_2$), pyrimidine-2-thione (pymSH), and pyridine-2-thione (pySH) (Chart 1) are synthesized and structurally characterized. These complexes (**1–9**) as well as a few previously reported ones, namely, $[Ag_2(L\text{-}NH)_4(PPh_3)_2](NO_3)_2$, $[Ag(L\text{-}NMe)_2(PPh_3)](NO_3)$, and $[Ag(bzimSH)_2(PPh_3)_2](OAc)$ (**10–12**) (L-NH = 1,3-imidazolidine-2-thione; L-NMe = 1-methyl-3-imidazolidine-2-thione and $bzimSH_2$ = benz-imidazoline-2-thione)[43] have been evaluated for their *in vitro* antimicrobial activity against various microorganisms {Gram positive bacteria: *Staphylococcus aureus* (MTCC 740), methicillin resistant *Staphylococcus aureus* (MRSA) *Staphylococcus epidermidis* (MTCC 435), *Enterococcus faecalis* (MTCC 439), Gram negative bacteria *Shigella flexneri* (MTCC 1457), *Escherichia coli* (MTCC 119) and a yeast *Candida albicans* (MTCC 227). Apart from antimicrobial studies, as an extension of bioactivity, some studies are explored in the use of complexes for their anticancer activity against MG63 – a bone cancer cell line.

Results and discussion

Synthesis and IR NMR spectroscopy

In this section, comments regarding synthesis of complexes (Chart 2) and IR spectral studies are described. In a typical

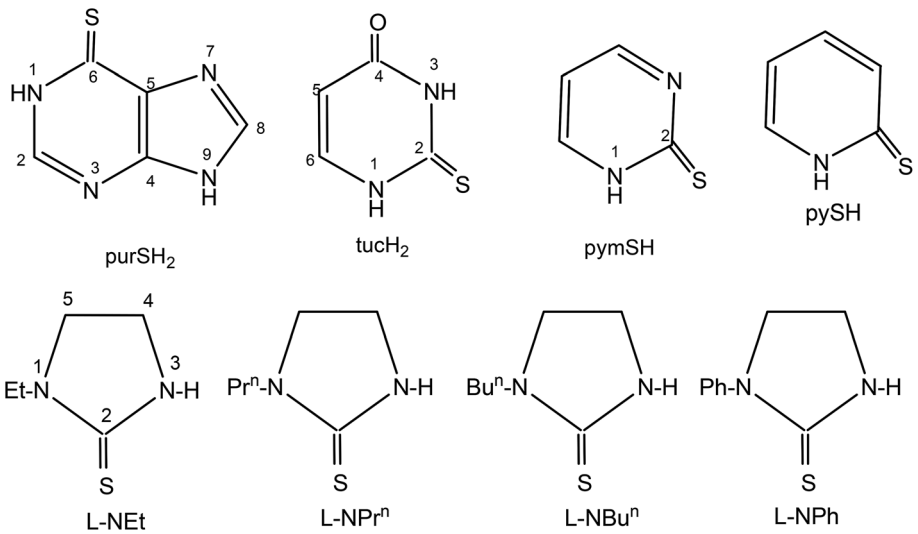

Chart 1 Thio-ligands used in the present investigation.

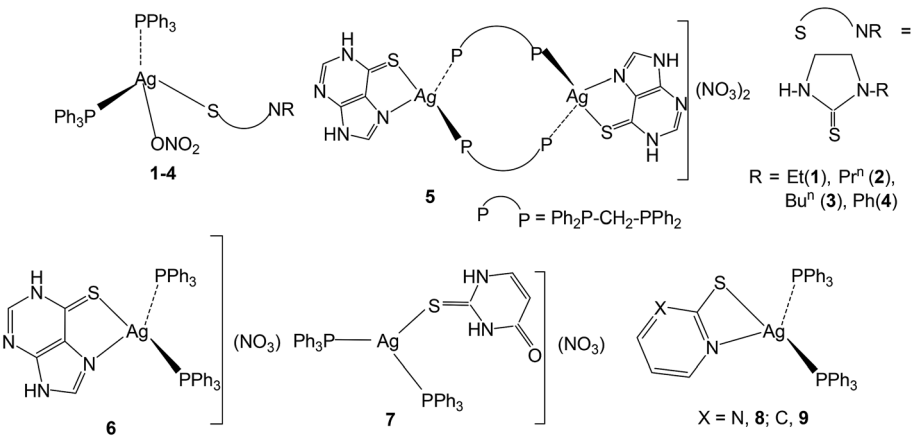

Chart 2 The structures of complexes, **1–9**.

reaction, to the solution of silver(I) nitrate in methanol was added two m mole of solid L-NEt ligand followed by stirring for 1 h, and to the clear solution was added two m mole of solid PPh_3 and the solution was further stirred for 15 minutes. The colorless contents were transferred into a culture tube for crystallization and after about one week crystalline product was obtained whose analytical data supported the composition as $[Ag(S\text{-}L\text{-}NEt)(PPh_3)_2(ONO_2)]$ **1**. Similarly, other complexes, namely, $[Ag(S\text{-}L\text{-}NR)(PPh_3)_2(ONO_2)]$ (R = Pr^n, **2**; Bu^n, **3**; Ph, **4**) were synthesized and bonding established using X-ray crystallography (*vide infra*). The crystalline pale yellow complex, $[Ag_2(N,S\text{-}purSH_2)_2(dppm)_2](NO_3)_2$ **5**, was obtained using same procedure from a reaction of silver nitrate with purine-6-thione ($purSH_2$) and bis(diphenylphosphino)methane (dppm). Complexes $[Ag(N,S\text{-}purSH_2)(PPh_3)_2](NO_3)$ **6**, $[Ag(S\text{-}tucH_2)(PPh_3)_2](NO_3)\cdot H_2O$ **7** and. $[Ag(L)(PPh_3)_2]$ (L = N,S-pymS, **8**; N,S-pyS **9**) were prepared from the reactions of silver(I) nitrate with two m mole of solid PPh_3 in methanol and the respective thio-ligands, $purSH_2$, $tucH_2$, pymSH and pySH with the only difference in case of the latter two complexes, where in Et_3N Lewis base was added.

The significant IR bands of complexes **1–9** are given in Table 1. The free thio-ligand, L-NEt shows ν(N–H) band of thioamide group at 3240 m, 3191 s cm^{-1}, which shifts to 3238 m, 3175 m cm^{-1} in complex **1**, and this shift supports that the thio-ligand L-NEt is coordinating to silver(I) ion as a neutral ligand. Similarly, low/high energy shift of ν(N–H) band of other thio-ligands, L-NPr^n, L-NBu^n, L-Ph, $purSH_2$, $tucH_2$, is noted in complexes **2–7** (see Table 1). However, the absence of ν(N–H) band in complexes **8** and **9** shows that the thio-ligands (pymSH, pySH) in these two complexes are coordinating as anionic ligands ($pymS^-$, pyS^-). The presence of nitrate is recognized from the splitting of ν_3 mode in **1–4** complexes which reveal coordination by nitrate and its lack of splitting in **5–7** complexes reveal the presence of ionic nitrate, which are supported by X-ray crystal structure determination. In literature,[60] four fundamental IR spectral bands due to the thioamide functional group, –N(H)–C(=S)–, classified as thioamide band I, near 1500 cm^{-1} {δ(N–H) + δ(C–H) + ν(C=N)}, thioamide band II in the region, 1200–1300 cm^{-1} {ν(C–N) + δ(N–H) + δ(C–H) + νC=S)}, thioamide band III, near 1000 cm^{-1} {ν(C–N)+ ν(C–S)}, and finally, thioamide band IV in the region, 700–850 cm^{-1} {ν(C–S)} were observed.[60] In complex **1**, thioamide bands III and IV (major contribution from νC–S + νC–N) underwent red shifts of 10 and 45 cm^{-1} respectively, whereas other two bands (I and II) remained less influenced (major contribution from δN–H + δC–H + νC=N + νC=S). It showed the thio-ligand, L-NEt, is binding to metal through sulfur only. Similar trends of these bands were seen in complexes **2–4** and **7** (see Table 1). Complexes **5**, **6**, **8** and **9** containing both Ag–S and Ag–N bonds have undergone a red shift of band I (16–50 cm^{-1}), slight blue shifts of bands II and III of 5–13 and 4–13 cm^{-1} respectively, while band IV undergoes red shift of 20–39 cm^{-1} with lowering of intensity. The appearance of $\nu(P\text{–}C_{Ph})$ bands in the region 1092–1095 cm^{-1} (weak to medium in intensity) confirm the presence of coordinated PPh_3 in the complexes **1–9**.

NMR spectroscopy

Proton NMR signals of coordination compounds **1–9**, free thio-ligands and co-ligands (PPh_3, dppm) are given in Table 2. The thio-ligand, L-NEt, shows NH proton signal at 6.39 ppm which significantly shifted to low field at 9.25 ppm in its complex **1** and this shift suggests that the thio-ligand is coordinating to the silver(I) ion through its S-donor atom, as a neutral ligand. The ring and side chain protons, C^4H_2, C^5H_2 and N–CH_2 of thio-ligand L-NEt showed an unresolved multiplet at 3.59(m; 6H), while –CH_3 proton signal occurred at 1.14 ppm as a triplet. In complex **1**, the C^4H_2, C^5H_2 and N–CH_2 proton signals were partially resolved into two multiplets, one at 3.72 ppm due to ring protons (4H, C^4H_2/C^5H_2) in the low field region and another at 3.59 (m; 2H, N–CH_2), while –CH_3 signal at 1.21 ppm (t; 3H, CH_3) shifted to a little high field region. The proton NMR signal of the thio-ligand and PPh_3 suggest coordination to silver through S and P donor atoms of the respective ligands. In other similar complexes **2–4**, the –NH protons signals at 5.91, 6.02 and 6.38 ppm shifted significantly to low fields at 7.87, 8.40 and 9.40 ppm respectively. Other ring, N-R side chain and PPh_3 phenyl ring protons all showed variable trends in complexes **2–4** relative to the un-coordinated ligands (Table 2).

Purine-6-thione has shown NMR signals at 13.70 ppm due to –N^1H– and –N^9H– protons, which marginally shifted to low field at 13.78 ppm in complex **6**, and likewise other two signals at

Table 1 IR spectral bands of complexes and free ligands[a,b,c]

Complex/free thio-ligand	ν(N–H)	ν(P–C_{Ph})	Band I	Band II	Band III	Band IV	NO_3^- bands[c]
[Ag(S-L-NEt)(PPh_3)$_2$](NO_3) **1**	3238 m 3175 m	1093 s	1507 s	1277 s	1027 m	747 w	ν_2, 834 w ν_3,1323 s, 1259 w ν_4, 722 s
Ag(S-L-NPr^n)(PPh_3)$_2$(κ^1:O–NO_2)] **2**	3051 m	1094 s	1509 m	1281 w	1027 m	745 s	ν_2, 851 w ν_3, 1384 s, 1349 m ν_4, (obscured by band IV)
Ag(S-L-NBu^n)(PPh_3)$_2$(κ^1:O–NO_2)] **3**	3183 m	1095 m	1518 s	1285 s	1029 w	747 s	ν_2, 858 w; ν_3, 1384 s, 1310 m; ν_4, (obscured by band IV)
[Ag(S-L-NPh)(PPh_3)$_2$](NO_3) **4**	3128 m	1094 s	1519 s	1244 s	1027 m	743 s	ν_2, 849 w ν_3, 1335 m, 1292 s ν_4, (obscured by band IV)
[Ag_2(N,S-purSH_2)$_2$(μ-dppm)$_2$]-(NO_3)$_2$ **5**	3259 m	1095 m	1507 m	1282 m	1027 w	748 m	ν_2, 858 w ν_3, 1382 m ν_4, 722 s
[Ag(N,S-purSH_2)(PPh_3)$_2$](NO_3) **6**	3133 w	1094 m	1479 m	1288 s	1026 w	743 m	ν_2, 852 m ν_3, 1384 s ν_4, 722 m
[Ag(S-tucH_2)(PPh_3)$_2$](NO_3) **7**	3139 m	1092 s	1565 s	1239 m	1001 w	723 w	ν_2, obscured ν_3, 1434 s ν_4, 723 w
[Ag(N,S-pymS)(PPh_3)$_2$] **8**	—	1092 m	1435 s	1270 w	1027 w	744 s	—
[Ag(N,S-pyS)(PPh_3)$_2$] **9**	—	1094 m	1480 m	1256 w	1027 w	723 w	—
L-NEt	3240 m, 3191 s	—	1513 s	1279 m	1037 m	792 m	—
L-NPr^n	3207 s	—	1514 s	1280 s	1037 w	806 w	—
L-NBu^n	3196 s	—	1514 s	1284 s	1041 w	803 w	—
L-NPh	3203 s	—	1518 s	1288 m	1040 m	757 s	—
purSH_2	3096 m	—	1529 m	1275 m	1014 m	782 w	—
tucH_2	3135 m	—	1567 s	1240 m	1004 w	761 w	—
pymSH	3186 w	—	1472 w	1275 s	1014 s	783 m	—
pySH	3162 s	—	1494 m	1255 m	1023 w	743 s	—
PPh_3	—	1088 s	—	—	—	—	—
dppm	—	1096 m	—	—	—	—	—

[a] See ESI for detailed spectral bands. s = strong, m = medium, w = weak. [b] Band I has contributions from δN–H + δC–H + νC=N; Band II has contributions from νC–N + δN–H + δC–H + νC=S; band III has contributions from νC–N + νC–S and band IV has contributions from νC–S. [c] ν_1 mode of nitrate could not be assigned owing to the bands of thio-ligand and PPh_3 ligand in this region.

8.33 and 8.14 ppm due to –C^8H and –C^2H groups shifted to low field at 8.40 and 8.30 ppm respectively, however, the magnitude of shift was very small. The purine-6-thione signals in complex **5** showed similar trend with respect to –N^1H/N^9H protons, but there was slightly up-field move with respect to the –C^8H and –C^2H protons. The 2-thiouracil showed proton NMR signals at 12.37, 7.36 and 5.78 ppm due to $N^{1,3}$H, C^6H and C^5H moieties and in complex **7** these shifted to 8.28, 7.13 and 5.55 ppm respectively. The pyrimidine-2-thione showed NMR signals due to –N^1H proton at 8.23 ppm which disappeared in its complex **8**, and signals due to C^4H, C^6H and C^5H protons showed mixed trend –low field/upfield in complex relative to the free thio-ligand. Similarly, in complex **9**, there was no signal due to –NH proton which was at 13.46 ppm in uncoordinated pySH (Table 2) and other signals due to C–H protons of thio-ligand showed minor variations in the same way as in case of complex **8**. Thus proton NMR clearly supported that thio-ligands pymSH and pySH were coordinating as anions in complexes **8** and **9**, while in other complexes, **1–7**, the thio-ligands were coordinating as neutral ligands.

The uncoordinated PPh_3 showed a multiplet at 7.32 ppm due to o-, m-, and p-H hydrogens of phenyl rings and in complexes **1–4**, **6–9**, this multiplet separated into ortho-hydrogen and meta-/para-hydrogen signals. For example, in complex **1** new multiplets appeared at low field, 7.52 ppm (m, o-H) and 7.40 ppm (m, m-and p-H). Other complexes **2–4**, **6–9** showed similar trends. In dppm complex **5**, the –CH_2– moiety shows a signal at 3.79 ppm which is low field relative to the –CH_2– moiety of free dppm, at 2.18 ppm. The phenyl ring protons of dppm are resolved into ortho, meta and para hydrogen signals in its complex **5**. Thus proton NMR shows coordination by PPh_3 and dppm in their complexes.

The ^{13}C NMR signals of silver(I) coordination compounds **1**, **3**, **5–8**, free thio-ligands and PPh_3/dppm co-ligands are given in Table 3. In complex **1**, the C^2 signal of thio-ligand L-NEt (179.9 ppm) has undergone a significant upfield shift relative to the free ligand (182.9 ppm). This shift indicates that the thio-ligand (L-NEt) is coordinating to silver(I) ion through S-donor atom and this leads to drift of electron density of nitrogen atoms with lone pairs towards C^2 carbon, leading to its enhanced shielding.

Table 2 ^{1}H NMR spectral data (δ in ppm) of complexes **1–9** and free ligands[a]

Complex/free thio-ligand	–NH protons	Ring protons of thio-ligand and co-ligands (PPh_3/dppm)
$[Ag(S\text{-}L\text{-}NEt)(PPh_3)_2(O–NO_2)]$[c] **1**	9.25 (s, 1H, NH)	3.72(m, 4H, C^4H_2/C^5H_2); 3.59 (q, 2H, N–CH_2); 1.21 (t, 3H, CH_3); 7.51 (m, 12H, o-H), 7.40 (m, 18H, m-H, p-H, PPh_3)
$[Ag(S\text{-}L\text{-}NPr^n)(PPh_3)_2(O–NO_2)]$[c] **2**	7.87 (s, 1H, NH)	3.48 (t, 2H, C^4H_2); 3.39 (t, 2H, N–CH_2,); 3.29 (t; 2H, C^5H_2); 1.51 (m; 2H, CH_2); 0.85 (t; 3H, CH_3); 7.32 (m, 12H, o-H), 7.23 (m, 18 H, m-H, p-H, PPh_3)
$[Ag(S\text{-}L\text{-}NBu^n)(PPh_3)_2(O–NO_2)]$[c] **3**	8.40 (s; 1H, N^3H)	3.62(dt; 2H, C^4H_2)[b]; 3.62 (dt; 2H, N–CH_2)[b]; 3.50 (t; 2H, C^5H_2);1.54 (quint; 2H, CH_2);1.35 (m; 2H, CH_2); 0.95 (t; 3H, CH_3); 7.39 (m, 12H, o-H), 7.33 (m, 18H, m-H, p-H, PPh_3)
$[Ag(S\text{-}L\text{-}NPh)(PPh_3)_2](NO_3)$[c] **4**	9.40 (s, 1H, NH)	4.18 (t, 2H, C^4H_2);3.86 (t, 2H, C^5H_2), 7.36 (m, 21H, o-H, p-H, PPh_3+ L-NPh)[e], 7.26 (m, 14H, m-H, PPh_3+ L-NPh)[d]
$[Ag_2(N,S\text{-}purSH_2)_2(\mu\text{-}dppm)_2]$ (NO_3)[c] **5**	13.78 (s, 2H, $N^{1,9}H$)	8.29 (s, 1H, C^8H); 7.73 (s, 1H, C^2H); 3.79 (s, 2H, P–CH_2–P, dppm), 7.36 (d, 8 H, o-H), 7.20 (t, 4H, p-H), 7.06 (t, 8H, m-H, dppm)
$[Ag(N,S\text{-}purSH_2)(PPh_3)_2](NO_3)$[c] **6**	13.78 (s, 2H, $N^{1,9}H$)	8.40 (s, 1H, C^8H); 8.33 (s, 1H, C^2H); 7.41(m, 12H, o-H), 7.27 (m, 18 H, m-H, p-H, PPh_3)
$[Ag(S\text{-}tucH_2)(PPh_3)_2](NO_3)$ [d] **7**	8.28 (s; 2H, $N^{1,3}H$)	7.13 (d; 1H, C^6H); 5.55 (d; 1H, C^5H); 7.37 (m, 12H, o-H), 7.25 (m, 18H, m-H, p-H, PPh_3)
$[Ag(N,S\text{-}pymS)(PPh_3)_2]$[d] **8**	—	7.85 (d; 2H, $C^{4,6}H$); 6.50 (t; 1H, C^5H); 7.34 (m, 12H, o-H), 7.24 (m, 18 H, m-H, p-H, PPh_3)
$[Ag(N,S\text{-}pyS)(PPh_3)_2]$[d] **9**	—	7.39 (t, 1H, C^3H); 7.24 (m, 1H, C^4H); 6.81 (t, 1H, C^5H); 7.57 (m, 13H, C^6H +o-H, PPh_3); 7.51 (m, 18H, m-H, p-H, PPh_3)
L-NEt[c]	6.39 (s, 1H, NH)	3.59(m, 6H, C^4H_2/C^5H_2/N–CH_2)[b];1.14 (t, 3H, CH_3)
L-NPr^n[,c]	5.91 (s, 1H, NH)	3.71 (t, 2H, C^4H_2); 3.58 (m, 2H, N–CH_2,); 3.46 (t, 2H, C^5H_2); 1.65 (m, 2H, CH_2); 0.97 (t, 3H, CH_3)
L-NBu^n[,c]	6.02 (s, 1H, NH)	3.64(m, 2H, C^4H_2)[b]; 3.53 (m, 4H, C^5H_2/N–CH_2)[b]; 1.53 (m, 2H, CH_2); 1.33 (m, 2H, CH_2); 0.91 (t, 3H, CH_3)
L-NPh[c]	6.38 (s, 1H, NH)	4.20 (t, 2H, C^4H_2); 3.76 (t, 2H, C^5H_2); 7.60 (m, 2H, o-H),7.42 (m, 2H, m-H), 7.27 (m, H, p-H)
$purSH_2$[d]	13.70 (s, 2H, $N^{1,9}H$)	8.33 (s, 1H, C^8H); 8.14 (s, 1H, C^2H)
$tucH_2$[d]	12.37 (s; 2H, $N^{1,3}H$)	7.36 (d; 1H, C^6H); 5.78 (d; 1H, C^5H)
pymSH[d]	8.23 (s; 1H, N^1H)	8.65 (d; 1H, C^4H); 7.32 (m; 1H, C^6H); 6.79 (t; 1H, C^5H)
pySH[d]	13.46 (s; 1H, N^1H)	7.6 (sb, 1H, C^6H); 7.35 (t; 1H, C^3H); 7.25 (t; 1H, C^4H);
6.69 (t; 1H, C^5H)		
PPh_3[c]	—	7.32 (m; o-H, m-H,p-H; 15H)
dppm[c]	—	2.18 (s; 2H, P–CH_2–P); 7.44 (m, 8H, o-H), 7.30 (m, 12H, m-H, p-H)

[a] See ESI for spectra. [b] (N–CH_2) and (ring proton C^4H_2 or C^5H_2) got merged. [c] $CDCl_3$. [d] DMSO. [e] N-Ph protons obscured by phenyl ring of PPh_3.

Similarly, in complexes **3** and **6**, the C^2 carbon signal has undergone upfield shift to 180.4 and 163.6 ppm, relative to the free ligands (L-Bu^n, $purSH_2$ = 183.4, 171.4 respectively). Complexes of purine-6-thione (**5**), 2-thiouracil (**7**) pyrimidine-2-thione (**8**) showed small lowfield shifts of C^2 carbon (171.6 **6**, 163.6 **7**, 183.2 **8** ppm), relative to the free ligands ($purSH_2$, $tucH_2$, pymSH = 171.4, 161.54, 181.9 ppm respectively). Further, the ring C^4, C^5 and side chain N-R carbons in complexes **1** and **3** as well as the $C^{4–6}$ carbons of complex **8** showed only minor variations as compared to the free thio-ligands. In complex **5**, the ring C^2 and C^4/C^8 carbon signals (145.9, 133.3 ppm) of $purSH_2$ have undergone up-field shift in complex **5** relative to the free ligand (152, 145 ppm), due to the deshielding of these carbons. Similar trends are seen in complex **7** in comparison to the free ligand $tucH_2$. The ipso, ortho, meta and para carbon signals of coordinated PPh_3 in complexes **1**, **3** and **6–8**, undergo variations as follows: (i) ipso-carbons have shown upfield shifts in all the complexes, ortho-carbons have shown upfield shifts in complexes **1**, **3**, **6**, **7** and lowfield shift in complex **8**, meta- and para-carbons showed only minor variations in either direction in all the complexes. Whereas, complex **5**, having dppm as a co-ligand, ipso-, and ortho- carbons showed upfield shift and meta-, para-carbons of P-Ph moiety along with carbon atoms of P–CH_2–P group have

Table 3 The ^{13}C NMR spectral data (δ in ppm) of complexes **1**, **3**, **5–8** and free ligands[a]

	Carbons of thio-ligands		Carbons of co-ligands (PPh_3/dppm)
Complex/free ligand	C^2/C^6	Other ring/chain carbons	i-C, o-C, m-C, p-C
$[Ag(S\text{-}L\text{-}NEt)(PPh_3)_2(O\text{–}NO_2)]$**1**[b]	179.9	48.26 (C^5), 42.06 (N–CH_2), 41.06(C^4), 12.23 (CH_3)	133.91 (i-C, J_{C-P} = 60 Hz), 132.47 (o-C, J_{C-P} = 135 Hz), 129.98 (p-C), 128.70 (m-C, J_{C-P} = 40 Hz)
$[Ag(S\text{-}L\text{-}NBu^n)(PPh_3)_2(O\text{–}NO_2)]$**3**[b]	180.4	48.80 (C^5), 46.72 (N–CH_2), 41.89 (C^4), 29.24 (CH_2), 19.88 (CH_2), 13.78 (CH_3)	133.87 (i-C, J_{C-P} = 70 Hz), 132.78 (o-C, J_{C-P} = 90 Hz), 130.01 (p-C), 128.80 (m-C, J_{C-P} = 35 Hz)
$[Ag_2(N,S\text{-}purSH_2)_2(\mu\text{-}dppm)_2](NO_3)_2$ **5**[c]	171.6	145.91(C^2), 133.34 (C^4/C^8), 128.75(C^5)	131.89 (i-C), 131.31 (o-C, J13C–P = 174 Hz), 128.93 (p-C), 128.74 (m-C, J_{C-P} = 52 Hz), 49.13 (CH_2)
$[Ag(N,S\text{-}purSH_2)(PPh_3)_2](NO_3)$ **6**[c]	163.6	152.75(C^2), 133.63 (C^4/C^8), 129.25(C^5)	132.60 (i-C, J_{C-P} = 8 Hz), 132.51 (o-C, J_{C-P} = 40 Hz), 129.37 (p-C), 129.25 (m-C)
$[Ag(S\text{-}tucH_2)(PPh_3)_2](NO_3)$ **7**[c]	163.6	164.92(C^4), 133.64 (C^6), 100.76(C^5)	132.60 (i-C, J_{C-P} = 12 Hz), 132.01 (o-C, J_{C-P} = 40 Hz), 129.36 (p-C), 129.24 (m-C)
$[Ag(N,S\text{-}pymS)(PPh_3)_2]$ **8**[c]	183.2	156.16(C^4H/C^6H), 114.16 (C^5H)	134.29 (i-C, J_{C-P} = 52 Hz), 133.88 (o-C, J_{C-P} = 68 Hz), 130.31 (p-C), 129.27 (m-C, J_{C-P} = 32 Hz)
L-NEt[b]	182.9	47.97 (C^5), 41.67 (N–CH_2), 41.39 (C^4), 12.21 (CH_3)	PPh_3[a]: 137.14 (i-C, J_{C-P} = 40 Hz), 133.83 (o-C, J_{C-P} = 76 Hz), 128.85 (p-C), 128.60 (m-C, J_{C-P} = 28 Hz)
L-NBu^n[,b]	183.4	48.61 (C^5), 46.77 (N–CH_2), 41.44 (C^4), 29.26 (CH_2), 19.99	
(CH_2), 13.89 (CH_3)	dppm[a]: 138.88 (i-C, J_{C-P} = 40 Hz), 132.92 (o-C, J_{C-P} = 84 Hz), 128.80 (p-C), 128.48 (m-C, J_{C-P} = 28 Hz),		
28.12 (CH_2)			
$purSH_2$[c]	171.4	152.08 (C^2), 145.04 (C^4/C^8), 128.76 (C^5)	—
$tucH_2$ [c]	161.5	176.17 (C^4), 142.63 (C^6), 106.80 (C^5)	—
pymSH [c]	181.9	154.69 (C^6), 159.08 (C^4), 110.01 (C^5H)	—

[a] See ESI for spectra. [b] $CDCl_3$. [c] DMSO.

shown low field shift relative to the free co-ligand. All these variations showed that it is the ipso carbon that is most affected in all the coordination compounds and hence the coordination of the PPh_3 to the silver(I) is through P donor atom. This upfield shift is attributed to electromeric effect involving movement of p-C and m-C phenyl ring electrons towards i-C–P bond axis leading to shielding of this carbon. The ^1J (^{13}C–^{31}P) coupling constant did not show regular trend.

Molecular structures

The crystal data of complexes **2**, **3**, **5–8** are given Table 4 which is placed in the experimental section, and their important bond parameters are given in Table 5. Complexes **3**, **5** and **6** crystallized in monoclinic crystal system in space groups $P2_1/c$ (**3**), $C2/c$ (**5**) and $P2_1/n$ (**6**), while each of complexes **2**, **7** and **8** crystallized in triclinic crystal system in space group $P\bar{1}$.

The molecular structures of complexes, $[Ag(S\text{-}L\text{-}NPr^n)(PPh_3)_2(O\text{–}NO_2)]$ **2**, and $[Ag(S\text{-}L\text{-}NBu^n)(PPh_3)_2(O\text{–}NO_2)]$ (**3**) are given in Fig. 1 and 2 respectively. In complex **2**, silver(I) is bonded to one S donor atom of the L-NPr^n thio-ligand, two P donor atoms of PPh_3 ligands and one O donor atom of a nitrate ion at bond distances of 2.6161(13) (S), 2.4552(11), 2.4450(11) (P) and 2.496(4) (O) Å respectively (Table 5). The corresponding bond distances of complex **3** are 2.5340(7)(S), 2.4524(6), 2.4554(6) (P) and 2.4999(19)(O), respectively. These bond distances are less than the sum of the covalent radii of the silver atom and the donor group (Ag–S, 3.50, Ag–P, 3.55, Ag–O, 3.20 Å)[61] and thus bonds in these complexes are similar to those found in literature.[43] While Ag–P and Ag–O distances in two complexes are similar, the corresponding Ag–S distances are different. The *n*-butyl group at N atom of thio-ligand L-NBu^n with positive inductive effect appears to increase lewis basicity of this ligand, which makes relatively short Ag–S bond in complex **3** *versus* that in **2** where it is longer. The short Ag–S distance in **3** is followed by relatively longer C–S bond distance (1.695(6) Å, **2**; 1.708(3) Å, **3**). The differences in Ag–S bond distances in these two complexes are reflected in Ag–O distances which is marginally short in **2**. The O–N bond distances of ONO_2 group differ more and lie in the range, 1.175 to 1.284 Å, while those in complex **3**, these distances are 1.232(3) to 1.249(3) Å – short in complex **2** {1.175(7) Å}*versus* that in **3** {1.232(3) Å}. The bond angles around the Ag metal center are in the ranges 97–129° (**2**) and 101–123° (**3**) respectively, suggesting distorted tetrahedral geometry of these complexes. It

Table 4 Crystallographic data for complexes **2**, **3**, **5**–**8**

	2	**3**	**5**
Empirical formula	$C_{42}H_{42}AgN_3O_3P_2S$	$C_{43}H_{44}AgN_3O_3P_2S$	$C_{60}H_{56}Ag_2N_{10}O_8P_4S_2$
CCDC	1878467	1878471	1878472
M	838.65	852.68	1448.88
T/K	293(2)	173(2)	293(2)
λ Å	Cu-Kα, 1.54178	Mo-Kα, 0.71073	Cu-Kα, 1.54178
Crystal system	Triclinic	Monoclinic	Monoclinic
Space group	$P\bar{1}$	$P2_1/c$	$C2/c$
a (Å)	10.5641(6)	13.6628(4)	25.2895(7)
b (Å)	12.9718(7)	16.2436(5)	13.2208(2)
c (Å)	15.3593(8)	18.8410(6)	23.5888(7)
α (°)	77.698(4)	90	90
β (°)	82.402(4)	105.902(3)	125.671(4)
γ (°)	79.796(4)	90	90
V (Å^3)	2014.12(19)	4021.4(2)	6407.1(4)
Z	2	4	4
D_{calcd} (g cm^{-3})	1.383	1.408	1.502
μ (mm^{-1})	5.577	0.675	6.958
F(000)	864	1760	2944
Reflns collected	14 231	36 999	12 856
Unique reflns	7658 (R_{int} = 0.0443)	13 487 (R_{int} = 0.0418)	6067 (R_{int} = 0.0264)
Data/restraints/parameters	7658/0/480	13 487/0/479	6067/223/447
Reflecs with [$I > 2\sigma(I)$]	6347	9990	5309
Final R indices [$I > 2\sigma(I)$]	R_1 = 0.0548	R_1 = 0.0449	R_1 = 0.0383
	wR_2 = 0.1389	wR_2 = 0.0962	wR_2 = 0.1040
Final R indices (all data)	R_1 = 0.0668	R_1 = 0.0702	R_1 = 0.0467
	wR_2 = 0.1469	wR_2 = 0.1121	wR_2 = 0.1101
Largest diff. peak/hole e Å^{-3}	1.720 and −0.671	1.193 and −0.482	1.160 and −0.441

	6	**7**	**8**
Empirical formula	$C_{41}H_{34}AgN_5O_3P_2S$	$C_{40}H_{36}AgN_3O_5P_2S$	$C_{41}H_{37}AgN_2OP_2S$
CCDC	1878468	1878469	1878470
M	846.60	840.59	775.59
T/K	293(2)	293(2)	173(2)
λ, Å	Cu-Kα, 1.54178	Cu-Kα, 1.54178	Mo-Kα, 0.71073
Crystal system	Monoclinic	Triclinic	Triclinic
Space group	$P2_1/n$	$P\bar{1}$	$P\bar{1}$
a (Å)	9.2210(3)	12.5062(7)	10.1240(4)
b (Å)	25.4962(8)	13.1744(7)	13.4635(6)
c (Å)	17.0609(5)	15.1280(7)	14.1829(6)
α (°)	90	99.534(4)	77.466(4)
β (°)	100.830(3)	103.826(5	78.784(4)
γ (°)	90	114.897(5)	78.993(4)
V (Å^3)	3939.6(2)	2092.7(2)	1828.62(14)
Z	4	2	2
D_{calcd} (g cm^{-3})	1.427	1.334	1.409
μ (mm^{-1})	5.728	5.408	0.730
F(000)	1728	860	796
Reflns collected	16 236	15 670	21 420
Unique reflns	7485 (R_{int}, 0.0407)	7954(R_{int}, 0.0586)	12 042 (R_{int}, 0.0323)
Data/restraints/parameters	7485/0/482	7954/0/472	12 042/0/436
Reflecs with [$I > 2\sigma(I)$]	6025	6920	9569
Final R indices [$I > 2\sigma(I)$]	R_1 = 0.0464	R_1 = 0.0449	R_1 = 0.0393
	wR_2 = 0.1153	wR_2 = 0.1161	wR_2 = 0.1125
Final R indices (all data)	R_1 = 0.0608	R_1 = 0.0519	R_1 = 0.0575
	wR_2 = 0.1253	wR_2 = 0.1226	wR_2 = 0.1339
Largest diff. peak/hole e Å^{-3}	1.114 and −0.612	0.745 and −0.972	0.808 and −0.488

is found that O1–Ag–S angle is smallest, 97.59(13), while P–Ag–P angle is largest, 129.48(4). It is opposite in complex **3** and these differences are attributed to the steric effect of R groups at N atoms of L-NR moiety.

Purine-6-thione chelates to Ag(I) in complex [Ag(N,S-purSH_2)(PPh_3)$_2$](NO_3) **6** (Fig. 3), through its N^7, S-donor atoms with Ag–N^7 and Ag–S bond distances of 2.468(4) and 2.6478(10) Å respectively. The Ag–P bond distances of 2.4511(8), 2.4301(9)

Table 5 Bond lengths (Å) and bond angles (°) of complexes 2, 3, 5–8

Mononuclear complexes							
	2	3		6	8	7	
Ag–S	2.6161(13)	2.5340(7)	Ag–S	2.6478(10)	2.5502(6)	Ag–S	2.5464(9)
Ag–O	2.496(4)	2.4999(19)	Ag–N	2.468(4)	2.579(2)	Ag–P	2.4531(7)
Ag–P	2.4552(11)	2.4524(6)	Ag–P	2.4511(8)	2.4477(6)	Ag–P	2.4787(8)
Ag–P	2.4450(11)	2.4554(6)	Ag–P	2.4301(9)	2.4528(6)	S–C	1.688(3)
S–C	1.695(6)	1.708(3)	S–C	1.693(4)	1.722(3)	O1–N	1.264(5)
O1–N	1.175(7)	1.232(3)	O1–N	1.200(6)	—	O2–N	1.227(5)
O2–N	1.284(7)	1.249(3)	O2–N	1.218(6)	—	O3–N	1.235(6)
O3–N	1.227(7)	1.233(3)	O3–N	1.240(5)	—	—	
			O–N–O	117.9(5), 121.8(5), 120.1(5)			
P–Ag–S	109.64(4)	114.81(2)	P–Ag–S	101.23(3)	115.58(2)	P–Ag–S	119.40(3)
P–Ag–S	108.08(4)	108.88(2)	P–Ag–S	120.37(3)	118.61(2)	P–Ag–S	110.51(3)
P–Ag–O1	98.00(12)	101.72(5)	P–Ag–N	108.14(10)	105.16(5)	P–Ag–P	124.53(2
P–Ag–O1	109.00(12)	102.46(2)	P–Ag–N	105.28(9)	106.64(5)	O–N–O	119.5(4)
O1–Ag–S	97.59(13)	103.09(6)	N–Ag–S	79.87(9)	61.89(5)	O–N–O	121.7(5)
P–Ag–P	129.48(4)	122.73(2)	P–Ag–P	130.17(3)	125.17(2)	O–N–O	118.8(4)

Dinuclear complex 5							
Ag–S	2.7239(9)	S–C; Ag⋯Ag	1.685(3) 3.466 (4)	P–Ag–S	124.79(3)	P–Ag–N	94.06(6)
Ag–P	2.4273(6)	O1–N	1.242(6)	P– Ag–S1	91.39(2)	S– Ag–N	77.27(7)
Ag–P	2.4677(7)	O2–N	1.224(7)	P– Ag–N	97.98(6)	P– Ag–P	143.54(2)
Ag–N	2.553(3)	O3–N	1.264(6)	O–N–O	122.1(6)	120.7(5)	117.1(6)

(P) Å are similar to those found in complex **2**. The nitrate NO_3^- ion is not coordinated in complex **6** with O–N bond distances of 1.200(6), 1.218(6) and 1.240(5) Å. It is noted that the average O–N distance of 1.219 (6) Å in complex **6** is less than the similar average O–N distances of 1.229(7) Å in complex **2** and 1.238(3) Å in complex **3**. The difference is obviously due to the coordinated nitrate in **2** and **3**, and ionic in complex **6** (Fig. 3). The N^7–Ag–S bite angle of 79.87(9)° is smallest, while P–Ag–P angle of 130.17(3)° is the largest among angles around the Ag atom. The geometry is severely distorted from the tetrahedron.

When dppm was used in place of PPh_3, purine-6-thione with silver(I) nitrate has yielded a P,P-bridged dinuclear complex,

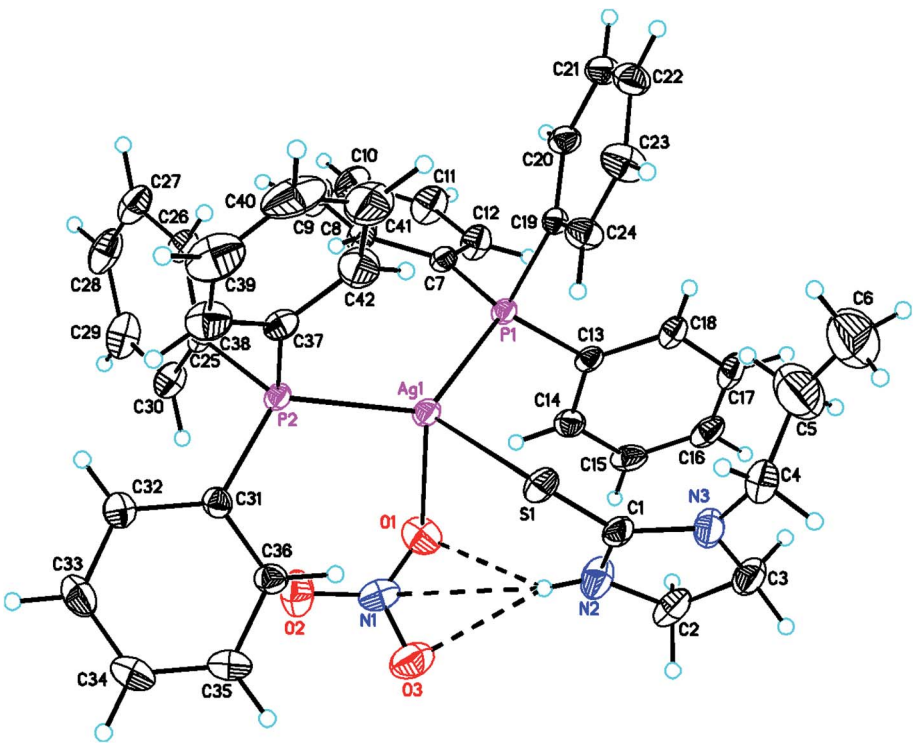

Fig. 1 Molecular structure of complex [Ag(S-L-NPr^n)$(PPh_3)_2(ONO_2)$] **2**.

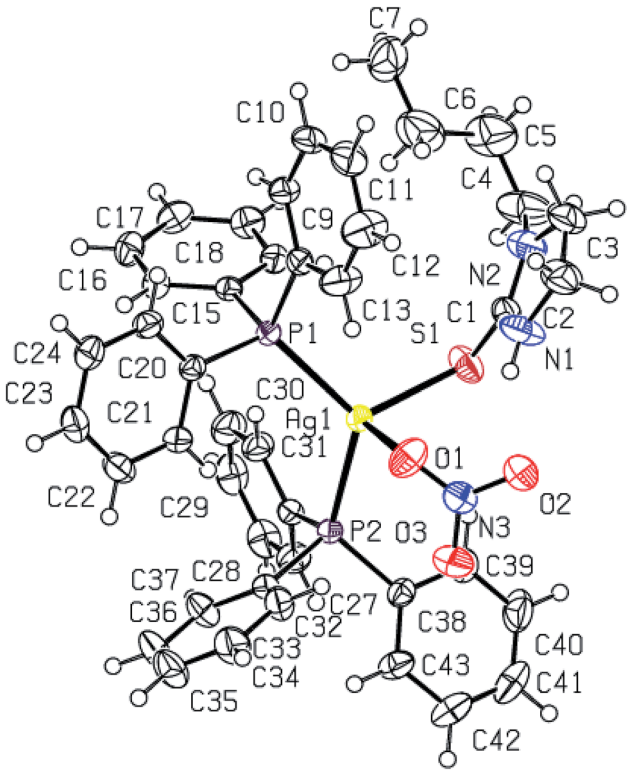

Fig. 2 Molecular structure of complex [Ag(S-L-NBu^n)(PPh$_3$)$_2$(ONO$_2$)] **3**.

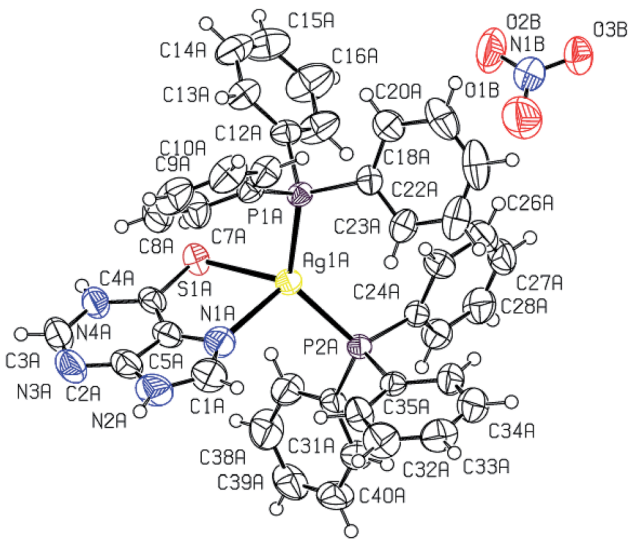

Fig. 3 Molecular structure of complex [Ag(N,S-purSH$_2$)(PPh$_3$)$_2$](NO$_3$) **6**.

[Ag$_2$(N,S-purSH$_2$)$_2$(μ-P,P-dppm)$_2$](NO$_3$)$_2$·2H$_2$O **5** (Fig. 4). The thio-ligand purSH$_2$ is chelating through its N,[7] S-donor atoms with relatively longer, Ag–S and Ag–N bond distances of 2.7239(9) and 2.553(3) Å respectively as compared with that of mononuclear complex **6** (Table 4), the Ag–P distances are however comparable in complexes **5** and **6**. The nitrates are lying outside the coordination sphere of silver metal ion. The angles around Ag vary from 77.27(7) to 143.54(2)° and thus geometry is severely distorted from tetrahedral geometry. The central core Ag$_2$P$_4$C$_2$ of complex **5** forms an eight membered ring with Ag···Ag contact distance of 3.466 Å which is close to twice the sum of radius of silver(I) ion, *viz.*, 3.4 Å.[61]

2-Thiouracil has formed a three coordinate complex, [Ag(S-tucH$_2$)(PPh$_3$)$_2$](NO$_3$)·H$_2$O **7**. Here, silver(I) is bonded to one S donor atom at Ag–S distance of 2.5464(9) Å and two P-donors at Ag–P bond distances of 2.4531(7) and 2.4787(8) Å (Fig. 5). The angles around the central silver atom in the range of 110–124° suggest distorted trigonal planar arrangement. The nitrate is lying outside the coordination sphere. The pyrimidine-2-thione ligand chelates to the silver atom as an anionic ligand through its N^1, S– donor atoms in [Ag(N,S-pymS)(PPh$_3$)$_2$] **8** (Fig. 6). Here, the Ag–S bond distance {2.5502(6) Å} is smaller than that found in the analogous complex [Ag(S-pymSH)(PPh$_3$)$_2$]NO$_3$, owing to pyrimidine-2-thione as anionic ligand in former complex *versus* neutral ligand in the latter complex.[23] Other bond distances, namely, Ag–P and Ag–N bond distances are in same trend as found in complex **6** with Ag–N bonds. The angles around Ag vary in the range, 61–125° with N–Ag–S bite angle of 61.89(5) and P–Ag–P bond angle of 125.17(2)° suggesting distorted tetrahedral geometry of complex **8**. The C–S bond lengths in complexes **2**, **3**, **5–8** fall in the range 1.68–1.72 Å, and are less than the C–S single bond length (1.81 Å) but longer than the C=S double bond length (1.62 Å), suggesting a partial double bond character in the C–S bonds in complexes.[61]

ESI-mass studies. The ESI-mass spectra of some selected complexes (**1–5**) was recorded and four types of species were identified (shown in Chart 3). Where type A species is, [Ag(L)(PR)]$^+$ (**1–5**) {L = L-NEt (**1**), L-NPr^n (**2**), L-NBu^n (**3**), L-NPh(**4**); PR = PPh$_3$ (**1–4**), dppm (**5**)}, type B species is, [Ag(L-NR)$_2$]$^+$ (**1–4**) {R = Et (**1**), Pr^n (**2**), Bu^n (**3**), Ph(**4**)}, type C species is, [Ag(PR)$_2$]$^+$ (**1–5**) {PR = PPh$_3$ (**1–4**), dppm (**5**)} and type D species is, [Ag(PR)]$^+$ (**5**) (PR = dppm). Molecular ion species were not shown by these complexes and all of the complexes have shown loss of a nitrate ion (see ESI, Fig. S60–S73†).

Antimicrobial studies

Silver complexes with imidazolidine-2-thiones and benzimidazoline-2-thione. Silver complexes of imidazolidine-2-thiones and benzimidazoline-2-thione, namely, **1–4**, **10–12** have shown bio-activity against Gram positive bacteria methicillin resistant *Staphylococcus aureus* (MRSA) with zone of inhibition values (zoi) in the range 14–30 mm. Complexes **1** and **4** have lower activity (22–23 mm zoi) but their MIC (10 μg mL^{-1}) value is same as that of gentamicin. In contrast, complex **10** has same activity as that of the standard drug gentamicin (33 mm zoi), with low MIC value (5 μg mL^{-1}) (Tables 6 and 7). The activity of analogous silver halide complexes of imidazolidine-2-thiones was found to be in a lower range, 15–25 mm zoi.[44] Further, all of these complexes, except complex **12**, were found to be active against Gram positive bacteria *Staphylococcus aureus* (MTCC 740) with zoi values in the range 12–24 mm. The activity of complexes **1**, **10** and **11** was comparable (22–24 mm zoi) to that of gentamicin (26 mm zoi) but their MIC values were somewhat high (Table 7). The activity of silver nitrate complexes is comparable to that of analogous silver halide complexes.[44]

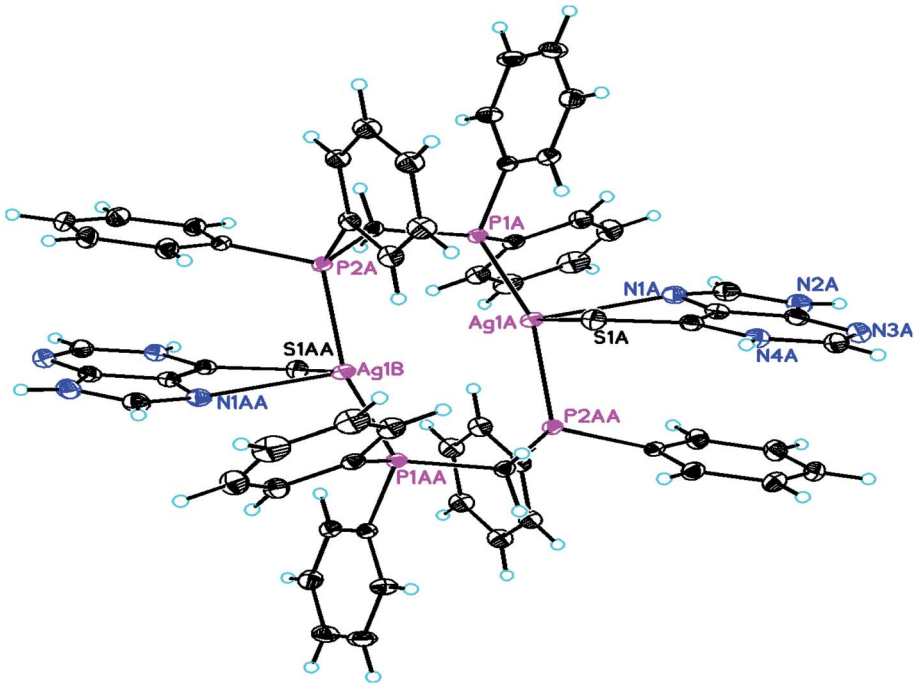

Fig. 4 Molecular structure of dinuclear complex $[Ag_2(N,S\text{-}purSH_2)_2(\mu\text{-}P,P\text{-}dppm)_2]\text{-}(NO_3)_2$ **5**.

Further, it is interesting to note that complexes **1**, **2** and **11** have shown activity of 24 mm (**2**) and 30 mm (**1**, **11**) against Gram positive bacteria *Staphylococcus epidermidis* (MTCC 435), with low MIC values (5–10 μg mL^{-1}) in comparison to the standard drug gentamicin with low activity and high MIC (zoi = 25 mm; MIC, 30 μg mL^{-1}).

Complexes **1–3**, **10** and **11** have shown activity against the microorganism Gram positive bacteria *Enterococcus faecalis* (MTCC 439) in the range 22–34 mm. Significantly, three complexes (**2**, **3** and **11**) have more activity (zoi, 30–34 mm) with low MIC values (1–7 μg mL^{-1}) than that of gentamicin (zoi, 27 mm, 30 μg mL^{-1}). The antimicrobial activity against Gram negative bacteria *Shigella flexneri* (MTCC 1457) in the range 19–24 mm (zoi) has been shown by the complexes **1**, **3**, **4** and **11** with MIC values in the range 7–50 μg mL^{-1}. This activity is lower than that shown by the standard drug (zoi, 34.5 mm, MIC, 5 μg mL^{-1}). Complexes **1**, **2**, **10** and **11** are active against yeast

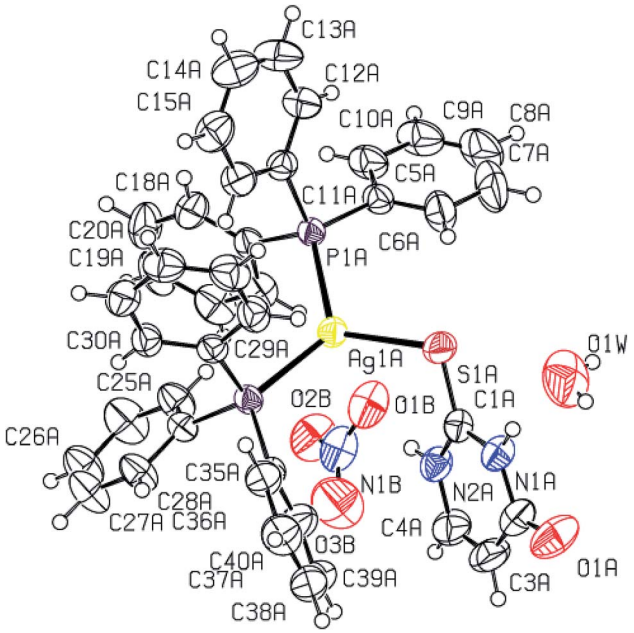

Fig. 5 Molecular structure of complex $[Ag(S\text{-}tucH_2)(PPh_3)_2](NO_3)$ **7**.

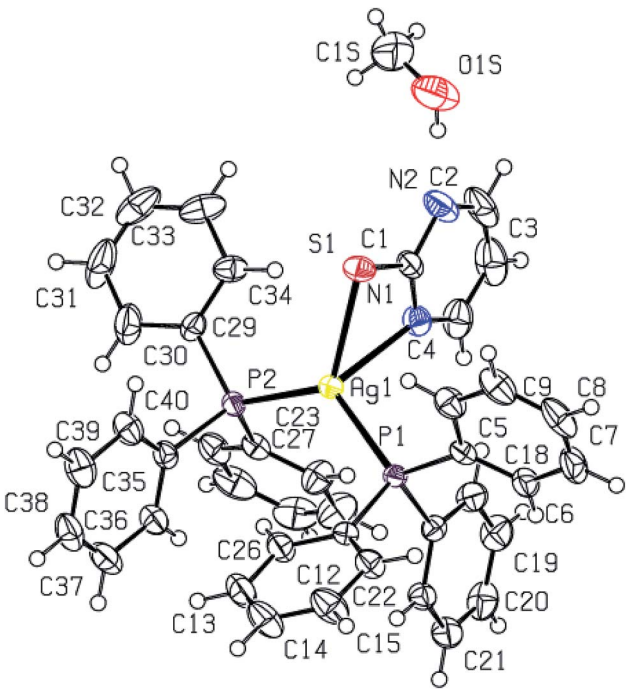

Fig. 6 Molecular structure of complex $[Ag(N,S\text{-}pymS)(PPh_3)_2]\cdot CH_3OH$ **8**.

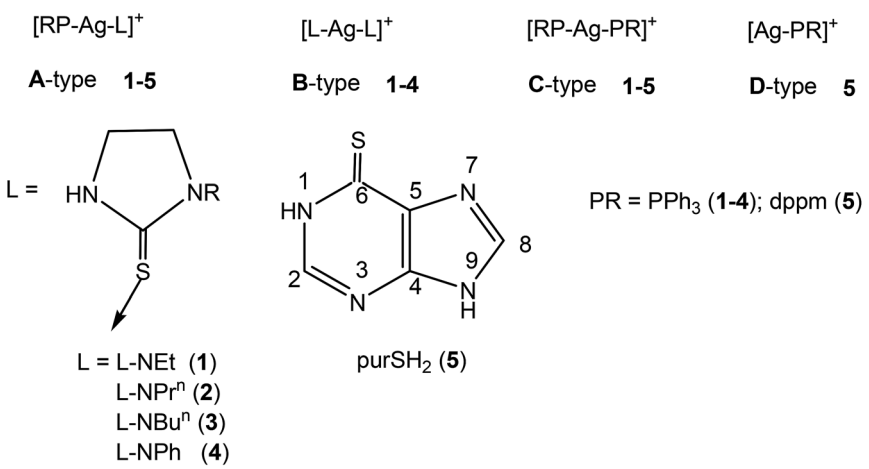

Chart 3 Common species found in mass-spectra of complexes.

Candida albicans (MTCC 227) (21–26 mm) with MIC values in the range 5–50 μg mL^{-1}. This activity is lower than that of the standard drug amphotericin B (zoi, 34 mm; MIC, 0.1 μg mL^{-1}). Only one complex showed activity of 26 mm with MIC value of 5 μg mL^{-1}, which is relatively close to that of the reference compound. Finally, it is added here that these complexes are more active as compared with the uncoordinated thio-ligands.

Silver complexes with purine-6-thione and related ligands. Silver complexes **5–9** have shown activity against Gram positive bacteria methicillin resistant *Staphylococcus aureus* (MRSA) in

Table 6 Antimicrobial activity of complexes **1–12**[a,b,c]

Complex/free thio-ligand/standard drug	MRSA[e]	*S. aureus*[f]	*S. epidermidis*[g]	*E. faecalis*[h]	*S. flexneri*[i]	*C. albicans*[j]
Imidazolidine-2-thione (1–4, 10, 11) and benzimidazoline-2-thione (11) complexes						
$[Ag(S\text{-}L\text{-}NEt)(PPh_3)_2(O\text{–}NO_2)]$ **1**	23	22	30	23	19	22
$[Ag(S\text{-}L\text{-}NPr^n)(PPh_3)_2(O\text{–}NO_2)]$ **2**	24	20	24	30	13	21
$[Ag(S\text{-}L\text{-}NBu^n)(PPh_3)_2\text{-}(ONO_2)]]$ **3**	14	13	15	30	23	14
$[Ag(S\text{-}L\text{-}NPh)(PPh_3)_2(O\text{–}NO_2)]$ **4**	22	19	20	19	24	18
$\{[Ag_2(L\text{-}NH)_4(PPh_3)_2](NO_3)_2$ **10**	30	24	21	22	15	26
$[Ag(S\text{-}L\text{-}NMe)_2(PPh_3)](NO_3)$ **11**	25	23	30	34	20	24
$[Ag(S\text{-}bzimSH)_2(PPh_3)_2]$ (OAc) **12**	17	NA	12	NA	NA	13
L-NH	NA	NA	NA	NA	15	NA
L-NMe	NA	NA	13	12	NA	NA
L-NEt	NA	NA	13	12	NA	NA
L-NPr^n	NA	NA	13	12	NA	NA
L-NBu^n	12	NA	NA	12	NA	NA
L-NPh	NA	NA	13	12	NA	NA
BzimSH	15	15	NA	NA	16	13
PPh_3	NA	NA	NA	NA	NA	NA
Purine-6-thione, 2-thiouracil, pyrimidine-2-thione and pyridinr-2-thione complexes (6–9)						
$[Ag_2(N,S\text{-}purSH_2)_2(\mu\text{-}dppm)_2]\text{-}(NO_3)2$ **5**	13	12	12	NA	NA	17
$[Ag(N,S\text{-}purSH_2)(PPh_3)_2]\text{-}(NO_3)$ **6**	15	12	14	NA	NA	18
$[Ag(S\text{-}tucH_2)(PPh_3)_2](NO_3)$ **7**	20	14	14	NA	26	20
$[Ag(N,S\text{-}pymS)(PPh_3)_2]$ **8**	12	NA	NA	NA	NA	13
$[Ag(N,S\text{-}pyS)(PPh_3)_2]$ **9**	20	NA	14	13	NA	18
$purSH_2$	18	13	NA	NA	NA	NA
$tucH_2$	19	16	NA	NA	NA	12
PymSH	19	17	17	NA	20	23
PySH	20	19	18	NA	14	30
dppm	NA	NA	NA	NA	NA	NA
Gentamicin[d,k]	33[d]	26[d]	25[d]	27[d]	34.5[d]	—
Amphotericin B[d,k]	—	—	—	—	—	34[d]

[a] All measurements are in mm diameter of the inhibition zone (N.A. indicates no activity). [b] The standard deviation varied in the range 0–1 based on three readings. [c] Studies were made in DMSO. [d] Commercially available antimicrobial agents. [e] MRSA. [f] *Staphylococcus aureus*. [g] *Staphylococcus epidermidis*. [h] *Enterococcus faecalis*. [i] *Shigella flexneri*. [j] *C. albicans*. [k] Gentamicin acts as positive control against bacteria (MRSA, *S. aureus, S. epidermidis, E. faecalis, S. flexneri*) and amphotericin B acts as positive control against yeast, *C. albicans*.

Table 7 Minimum inhibitory concentration (μg mL^{-1}) of silver(I) complexes **1–12**[a,b]

Complex/standard drug	MRSA	*S. Aureus*	*S. epidermidis*	*E. faecalis*	*S. flexneri*	*C. albicans*
Imidazolidine-2-thione (1–4, 10, 11) and benzimidazoline-2-thione (11) complexes						
1	10	10	5	10	50	50
2	50	50	10	7	ND	1010 10
3	ND	ND	1000	1	7	ND
4	10	500	50	500	10	750
10	5	10	50	50	1000	5
11	7	10	7	1	50	10
12	7	ND	ND	ND	ND	ND
Purine-6-thione, 2-thiouracil, pyrimidine-2-thione and pyridinr-2-thione complexes (6–9)						
5	ND	ND	ND	ND	ND	50
6	1250	ND	ND	ND	ND	50
7	50	ND	ND	ND	7	10
8	ND	ND	ND	ND	ND	ND
9	50	ND	ND	ND	ND	50
Gentamicin	10	0.5	30	30	5	—
Amphotericin B	—	—	—	—	—	0.1

[a] MIC in μg mL^{-1}. [b] ND-not determined.

the range 12–20 mm. In comparison to the activity of thio-ligands, it was found that the free purine-6-thione ($purSH_2$; zoi = 18 mm) and pyrimidine-2-thione (pymSH; zoi = 19 mm) ligands were found to be more active than their complexes, **5**, **6** and **8**. Further, the activity of free 2-thiouracil ($tucH_2$, zoi = 19 mm) and pyridine-2-thione (pySH, zoi = 20 mm) ligands was found to be same as that of their corresponding complexes **7** and **9**, respectively. The activity of complexes **5** and **6** against Gram positive bacteria *Staphylococcus aureus* (MTCC 740) was found to be similar to that of the free purine-6-thione (zoi = 13 mm). Further, the activity of $tucH_2$ (16 mm) was found to be more than that of its complex **7**. On the other hand, while uncoordinated pymSH and pySH were active (zoi = 17 mm and 19 mm respectively), but their complexes **8** and **9** were inactive against Gram positive bacteria *Staphylococcus aureus* (MTCC 740) . Unlike lack of literature reports about activity of silver complexes against MRSA, there is one report of activity of related complex of pyrimidine-2-thione, namely, $[Ag(S\text{-}pymSH)(PPh_3)]NO_3$ against *Staphylococcus aureus*.[23] The uncoordinated thio-ligands, $purSH_2$ and $tucH_2$ were inactive against Gram positive bacteria *Staphylococcus epidermidis* (MTCC 435), while their complexes **5**, **6** and **7** showed low activity (zoi = 12–14 mm). Further, free pymSH was active (zoi = 17 mm) against *Staphylococcus epidermidis* but its complex **8** was inactive. Similarly, pySH was more active (zoi = 18 mm) than its complex **9** (zoi = 14 mm).

Only complex **9** showed activity (zoi = 13 mm) against Gram positive bacteria *Enterococcus faecalis* (MTCC 439), while other complexes and free ligands were inactive. Among the free thio-ligands, only pymSH and pySH showed activity of 20 and 14 mm (zoi) against Gram negative bacteria *Shigella flexneri* (MTCC 1457), but as regards their complexes, only 2-thiouracil complex **7** showed activity of 26 mm (zoi) which was somewhat close to that of standard drug gentamicin (zoi = 34.5 mm) (Table 7). Additionally, their MIC values were comparable (complex **7**, MIC = 7 μg mL^{-1}; gentamicin, MIC = 7 μg mL^{-1}). This is an interesting outcome of the study owing to the importance of $tucH_2$ derivatives in the development of metal based drugs.[62–64] Finally, as regards activity against the yeast *Candida albicans*, the thio-ligand $purSH_2$ was inactive, while its complexes **5** and **6** showed moderate activity of 17 mm (**5**) and 18 mm (**6**) respectively. Further, while free $tucH_2$ was inactive, its complex **7** was found to be active with (zoi = 20 mm). In contrast, the thio-ligands pymSH (23 mm) and pySH (30 mm) were found to be more active than their corresponding complexes **8** (13 mm) and

Table 8 OD values of silver complexes (**1**, **3**, **4**, **7**, **8**, **11**) at wavelength 590 nm

Complexes	OD values	Cell viability
$[Ag(L\text{-}NEt)(PPh_3)_2(O\text{–}NO_2)]$ **1**	0.237[a]	79.53%
$[Ag(L\text{-}NBu^n)(PPh_3)_2(O\text{–}NO_2)]$ **3**	0.224[a]	75.17%
$[Ag(L\text{-}NPh)(PPh_3)_2(O\text{–}NO_2)]$ **4**	0.288[a]	96.31%
$[Ag(tucH_2)(PPh_3)_2](NO_3)$ **7**	0.565[b]	84%
$[Ag(pymS)(PPh_3)_2]$ **8**	0.666[b]	99.10%
$[Ag(L\text{-}NMe)_2(PPh_3)](NO_3)$ **11**	0.271[a]	90.94%

[a] OD value of control = 0.298. [b] OD value of control = 0.672.

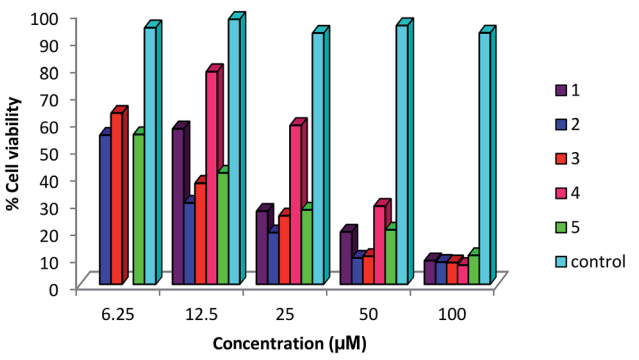

Fig. 7 Effect of concentration of complexes **1–5** on viability of MG 63 cells; untreated cells represent control.

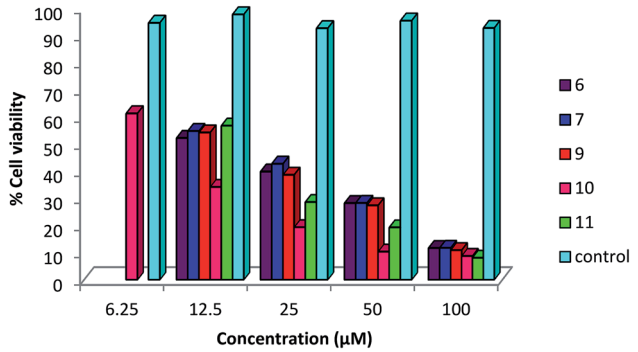

Fig. 8 Effect of concentration of complexes **6**, **7**, **9–11** on viability of MG 63 cancerous cells; where untreated cells represent control.

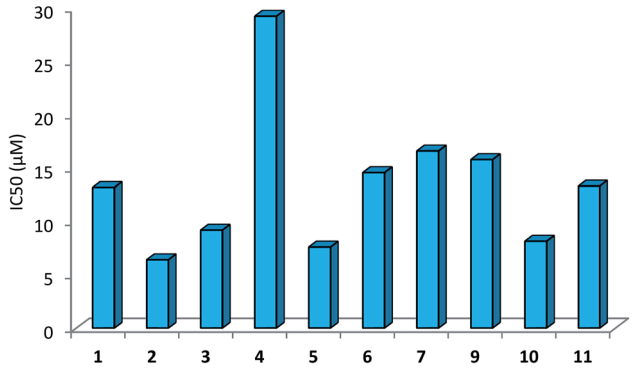

Fig. 9 Plot of IC_{50} values of complexes **1–6**, **7**, **9–11** against MG 63 cells.

9 (18 mm). Further, complex **9** was more active against *Candida albicans* than the reported analogous complex, $[Ag(S\text{-}pySH)_2(PPh_3)]NO_3$ with pyridine-2-thione (pySH) bonded as neutral ligand.[30]

Among these complexes, complex **7** showed MIC of 10 μg mL^{-1}, while all other complexes showed high MIC values. Complexes **5–9** and thio-ligands showed lower activity than the standard antibiotics, gentamicin and amphotericin B. This outcome of the study is consequence of systematic scanning of complexes for their antimicrobial activity and cell viability in view of scant reports in literature as highlighted in this paper.

Cellular toxicity using MTT assay. All the complexes (**1–12**) were tested for their *in vitro* toxicity using MTT assay. This cytotoxicity assay is based on the capacity of mitochondrial succinate dehydrogenase enzyme in blood cells to reduce the yellow water soluble substrate MTT into an insoluble purple formazan product which is measured spectrophotometrically. Interestingly, complexes $[Ag(S\text{-}L\text{-}NEt)(PPh_3)_2(O\text{–}NO_2)]$ **1**, $[Ag(S\text{-}L\text{-}NBu^n)(PPh_3)_2(O\text{–}NO_2)]$ **3**, $[Ag(S\text{-}L\text{-}NPh)(PPh_3)_2(O\text{–}NO_2)]$ **4**, $[Ag(S\text{-}tucH_2)(PPh_3)_2](NO_3)$ **7**, $[Ag(N,S\text{-}pymS)(PPh_3)_2]$ **8** and $[Ag(S\text{-}L\text{-}NMe)_2(PPh_3)](NO_3)$ **11** showed purple color with optical density (OD) of 0.237 (**1**), 0.224 (**3**), 0.288 (**4**), 0.271 (**11**) (control OD = 0.298), 0.565 (**7**) and 0.666 (**8**) (control = 0.672) respectively at 590 nm wavelength. The OD of the control (untreated cells in DMSO) was 0.872 (Table 8). Therefore these complexes were found to be non-cytotoxic with respective cell viability of 79.53% (complex **1**), 75.17% (complex **3**), 96.31% (complex **4**), 84% (complex **7**), 99.10% (complex **8**) and 90.94% (complex **11**).

Antitumor activity

A status of anti-cancer/tumor activity of complexes of silver(I) with heterocyclic-2-thiones is given in introduction,[17,18,36,38,39] and it was noted that the study pertained to *in vitro* cytotoxic activity against murine leukemia (L1210), human T-lymphocyte (Molt4/C8 and CEM) cells, breast cancer cell lines (MDA-MB-231, MCF-7), colon cancer cell line (HT-29), and leiomyosarcoma cancer cells (LMS). In this investigation, silver(I) complexes (**1–7**, **9–10**) with the thio-ligands, namely, *N*-substituted-imidazolidine-2-thiones, benzimidazoline-2-thione, purine-6-thione, pyridine-2-thione and 2-thiouracil have been studied for their *in vitro* antitumor activity against human bone cancer cell line MG63, using MTT [3-(4,5-dimethylthiazol-2-yl)-2, 5-diphenyl tetrazolium bromide] assay. The antitumor potential of these complexes was evaluated by exposing a fixed number of cancer cells to increasing concentration of complexes. Fig. 7 and 8 depict the effect of complex concentration on the death of the cancerous cells. As an example, complex **2** at concentrations of 6.25, 12.5, 25, 50 and 100 μM, showed the percent killing of cancerous cells up to 40, 65, 75, 85 and 91% respectively. Similar effect was observed when complexes **1**, **3–7**, **9–10** were studied against MG63 cancerous cells. Further, the cyto-toxic activity of complexes on cancerous cell line is interpreted on the basis of their IC_{50} (half maximal inhibitory concentration) values (Table 8). The IC_{50} values of different complexes and the free thio-ligands were calculated from the curves obtained between concentration of complexes and percentage viability of cancerous cells (Fig. 9).

The IC_{50} values of complexes **1–12** ranged between 6.42-29.22 μM (Table 9). Among the complexes tested, complexes, **2**, **3**, **5** and **10** have shown IC_{50} values of 6.42 (**2**), 9.21 (**3**), 7.62 (**5**) and 8.17 (**10**) μM respectively; other complexes **1**, **6**, **7**, **9** and **11**

Table 9 Anticancer activity of silver complexes (**1–7**, **9–11**) against human bone cancer MG63 cell line[a]

Complexes	IC_{50} (μM)		IC_{50} (μM)
$[Ag(L\text{-}NEt)(PPh_3)_2(O\text{–}NO_2)]$ **1**	13.20	$[Ag(N,S\text{-}purSH_2)(PPh_3)_2](NO_3)$ **6**	14.58
$[Ag(L\text{-}NPr^n)(PPh_3)_2(O\text{–}NO_2)]$ **2**	6.42	$[Ag(S\text{-}tucH_2)(PPh_3)_2](NO_3)$ **7**	16.61
$[Ag(L\text{-}NBu^n)(PPh_3)_2(O\text{–}NO_2)]$ **3**	9.21	$[Ag(N,S\text{-}pyS)(PPh_3)_2]$ **9**	15.80
$[Ag(L\text{-}NPh)(PPh_3)_2(O\text{–}NO_2)]$ **4**	29.22	$[Ag_2(L\text{-}NH)_4(PPh_3)_2]\text{-}(NO_3)_2$ **10**	8.17
$[Ag_2(N,S\text{-}purSH_2)_2(\mu\text{-}dppm)_2]\text{-}(NO_3)_2$ **5**	7.62	$[Ag(L\text{-}NMe)_2(PPh_3)](NO_3)$ **11**	13.33

[a] Ligands: L-NR, R = H, Me, Et, Pr^n. Bu^n and Ph; PPh_3: IC_{50} (μM) is >100; $purSH_2$, 24.78, $tucH_2$, 44.26 and pySH, 29.66.

have IC_{50} values in close range, 13.22 to 16.61 μM, and finally complex **4** lowest IC_{50} value of 29.22 μM. The free thio-ligands, L-NR (R = H, Me, Et, Pr, Bu, and Ph), purSH_2, tucH, and pymSH are either inactive or have low ant-cancer activity.

Conclusion

Coordination compounds of *N*-substituted 1,3-imidazolidine-2-thiones, purine-6-thione, 2-thiouracil, pyrimidine-2-thione and pyridine-2-thione with silver(I) nitrate have shown moderate to high antimicrobial bio-activity against methicillin resistant *Staphylococcus aureus* (MRSA), *Staphylococcus aureus*, *Staphylococcus epidermidis*, *Enterococcus faecalis* and yeast *Candida albicans.* Coordination compounds [Ag(S-L-NEt)$(PPh_3)_2$(O–NO_2)] **1**, [Ag(S-L-NPh)$(PPh_3)_2$(O–NO_2)] **4**, [Ag(S-tucH_2)$(PPh_3)_2$](NO_3) **7**, [Ag(N,S-pymS)$(PPh_3)_2$] **8** and [Ag(S-L-NMe)$_2(PPh_3)$](NO_3) **11** studied for their *in vitro* cell viability were found to be non-cytotoxic with respective cell viability of 79.53 (**1**), 96.31 (**4**), 84 (**7**), 99.10 (**8**) and 90.94% (**11**) respectively. Specifically complexes of *N*-substituted imidazoldine-2-thiones have shown unusual bio-activity against methicillin resistant *Staphylococcus aureus* (MRSA), *Staphylococcus epidermidis and Enterococcus faecalis* which rivals with gentamicin or even better in some cases. The anti-tumor study of silver complexes against human osteosarcoma cell line (MG63) has shown IC_{50} values in the range 6–33 μM. The activity of complexes is attributed to the enhanced lipophilic character of complexes, in comparison to silver nitrate which being soluble in water combines with chloride in body system forming insoluble AgCl, thus losing its bioactivity. However, presence of nitrate in ionic/coordinated forms in the present mixed ligand complexes of thio-ligands and co-ligands develop chemical environments which lead to their enhanced lipophilic character responsible for bioactivity. Future investigations might provide more light on mechanistic aspects. And *in vivo* studies are needed to explore their medicinal potential.

Experimental section

Chemicals and techniques

The thio-ligands, namely, purine-6-thione (purSH_2), pyrimidine-2-thione (pymSH), pyridine-2-thione (pySH), 2-thiouracil (tucH_2) and benz-imidazoline-2-thione (bzimSH_2) were procured from Sigma-Aldrich Ltd and used as such, whereas, other thio-ligands such as, imidazolidine-2-thione (L-NH), 1-methyl-imidazolidine-2-thione (L-NMe), 1-ethyl-imidazolidine-2-thione (L-NEt), 1-*n*-propyl-imidazolidine-2-thione (L-NPr^n), 1-*n*-butyl-imidazolidine-2-thione (L-NBu^n), and 1-phenyl-imidazolidine-2-thione (L-NPh) were prepared as per the literature methods.[65,66] Silver(I) nitrate was purchased from Sigma-Aldrich and used as received. Elemental analysis (C, H, N, S) were carried out using the Thermo Finnigan Flash technique. The melting points were determined with a Gallenkamp electrically heated apparatus. The IR spectra were recorded using KBr pellets on a Varian 660 FT IR Spectrometer in the 4000–400 cm^{-1} range. The $^1H/^{13}C$ NMR spectra were recorded in $CDCl_3$ and DMSO using Bruker Avance II 400 NMR spectrometer at 400 MHz and Bruker Ascend 500 NMR spectrometer at 500 MHz with TMS as an internal reference. The ESI-mass spectra were recorded in DMSO or $CHCl_3$ solvents using Bruker Daltonik LS-MS high resolution micro TOF-Q II 10356 spectrometer.

Synthesis of Silver(I) complexes

[Ag(L-NEt)$(PPh_3)_2(ONO_2)$] (1). To a solution of silver(I) nitrate (0.025 g, 0.15 mmol) in methanol (5 mL) was added solid 1-ethyl-imidazolidine-2-thione (0.038 g, 0.30 mmol) and the contents were stirred for a period of 1 h at room temperature. To the clear solution formed was added triphenylphosphine (0.076 g, 0.30 mmol) and slow evaporation of this solution at room temperature for a period of one week gave white crystalline solid of complex **1** (yield, 0.096 g, 80%, mp 87–90 °C). Elemental analysis for $AgC_{41}H_{40}N_3P_2SO_3$ (824): calcd C 59.72; H 4.85; N 5.10; S 3.88%; found: C 59.97; H 5.13; N 5.17, S 4.16%. Complex **4** was prepared similarly.

[Ag(L-NPr^n)$(PPh_3)_2(ONO_2)$] (2). To a solution of silver(I) nitrate (0.025 g, 0.15 mmol) in methanol (5 mL) was added solid 1-*n*-propyl-imidazolidine-2-thione (0.042 g, 0.30 mmol) and the contents were stirred for 1 h at room temperature. To the clear solution formed was added triphenylphosphine (0.076 g, 0.30 mmol). Slow evaporation of this solution at room temperature formed a white solid which after re-crystallization from methanol–toluene mixture (5 mL, 4 : 1, v/v) yielded colorless crystals of **2** (yield, 0.086 g, 70%, mp 153–156 °C). Elemental analysis for $AgC_{42}H_{42}N_3SP_2O_3$ (838.65): calcd C 60.09; H 5.00; N 5.00; S 3.81%; found: C 60.35; H 5.25; N 5.37, S 4.12.

[Ag(L-NBu^n)$(PPh_3)_2(ONO_2)$] (3). To a solution of silver(I) nitrate (0.025 g, 0.15 mmol) in methanol (5 mL) was added solid 1-*n*-butyl-1,3-imidazolidine-2-thione (0.046 g, 0.30 mmol) and the contents were stirred for 1 h at room temperature. To the clear solution formed was added triphenylphosphine (0.076 g, 0.30 mmol). Slow evaporation of this solution at room temperature formed a white solid which after recrystallization from dichloromethane and toluene mixture (5 mL, 4 : 1, v/v) yielded colorless crystals of **3** (yield, 0.093 g, 75%, mp 118–120 °C). Elemental analysis for $AgC_{43}H_{44}N_3SP_2O_3$ (852.68): calcd C 60.56; H 5.16; N 4.92; S 3.75%; found: C 60.77; H 5.56; N 5.06, S 3.67%.

[Ag(L-NPh)$(PPh_3)_2(ONO_2)$] (4). Colorless compound (yield, 0.099 g, 78%, mp 136–138 °C). Elemental analysis for $AgC_{45}H_{40}N_3SP_2O_3$ (873.24): calcd C 61.94; H 4.59; N 4.82; S 3.67%; found: C 62.29; H 4.82; N 4.89, S 4.01%.

[Ag_2(purSH_2)$_2$(dppm)$_2$](NO_3)$_2$·$2H_2O$ (5). To a solution of silver(I) nitrate (0.025 g, 0.15 mmol) in methanol (5 mL) was added a solution of purine-6-thione (0.025 g, 0.15 mmol) in methanol (5 mL), followed by stirring for 1 h at room temperature. To the yellow viscous solution thus formed was added solid bis(diphenylphosphino)methane (0.057 g, 0.15 mmol), followed by stirring until a clear solution was formed. Slow evaporation of the solution at room temperature gave pale yellow crystals of **5** (yield, 0.092 g, 87%, mp 150–152 °C). Elemental analysis for $Ag_2C_{64}H_{62}N_8P_4S_2O_8$ (1442.95): calcd C 49.72; H 3.87; N 9.66, S 4.41%; found: C 49.59; H 4.26; N 9.51, S 4.08%.

$[Ag(purSH_2)(PPh_3)_2](NO_3)$ (6). To a solution of silver(I) nitrate (0.025 g, 0.15 mmol) in methanol (5 mL) was added solid triphenylphosphine (0.076 g, 0.30 mmol) and the contents were stirred for 1 h at room temperature. To the clear solution formed was added a solution of purine-6-thione (0.025 g, 0.15 mmol) in methanol (5 mL) and slow evaporation of this solution at room temperature gave colorless crystals of **6** (yield, 0.077 g, 65%, mp 170–172 °C). Elemental analysis for $AgC_{41}H_{34}N_5P_2SO_3$ (846.60): calcd C 58.11; H 4.01; N 8.26; S 3.77%; found: C 57.73; H 4.15; N 8.26, S 3.73%.

$[Ag(tucH_2)(PPh_3)_2](NO_3)\cdot H_2O$ (7). To a solution of silver(I) nitrate (0.025 g, 0.15 mmol) in methanol (5 mL) was added solid triphenylphosphine (0.076 g, 0.30 mmol) and the contents were stirred for 1 h at room temperature. To the clear solution formed was added solid 2-thiouracil (0.037 g, 0.30 mmol) and slow evaporation of this solution at room temperature gave colorless crystals of **7** (yield 0.12 g, 92%, mp 116–118 °C). Elemental analysis for $AgC_{40}H_{36}N_3P_2SO_5$ (840): calcd C 57.10; H 4.28; N 4.99; S 3.80%; found: C 57.41; H 4.43; N 4.85, S 3.60%.

$[Ag(pymS)(PPh_3)_2](CH_3OH)$ (8). To a solution of silver(I) nitrate (0.025 g, 0.15 mmol) in methanol (5 mL) was added solid triphenylphosphine (0.076 g, 0.30 mmol) and the contents were stirred for 1 h at room temperature. To the clear solution formed was added a solution of pyrimidine-2-thione (0.016 g, 0.15 mmol) in methanol (5 mL) in presence Et_3N base (0.5 mL). The color of the reaction mixture became light yellow. Slow evaporation of this solution at room temperature gave pale yellow crystals of **8** (yield, 0.08 g, 72%, mp 85–88 °C). Elemental analysis for $C_{41}H_{37}AgN_2OP_2S$ (775.59): calcd C 63.43; H 4.77; N 3.61; S 4.12%; found: C 63.08; H 5.15; N 4.93, S 3.76%. Complex **9** was prepared similarly.

$[Ag(pyS)(PPh_3)_2]$ (9). Pale yellow compound (yield, 0.07 g, 65%, mp 56 °C). Elemental analysis for $C_{41}H_{34}AgNP_2S$ (742): calcd C 66.31; H 4.58; N 1.88; S 4.31%; found: C 66.63; H 4.86; N 1.98; S 4.51%.

Complexes 10–12.[43] Complexes, $[Ag_2(L\text{-}NH)_2(PPh_3)_2](NO_3)_2\cdot 2CH_3OH$ **10**, $[Ag(L\text{-}NMe)_2(PPh_3)](NO_3)$ **11**, and $[Ag(bzimSH)_2(PPh_3)_2](OAc)\cdot H_2O$ **12**, were prepared as reported (L-NH = 1,3-imidazolidine-2-thione; L-NMe = 1-methyl-3-imidazolidine-2-thione and $bzimSH_2$ = benz-imidazoline-2-thione).[43]

X-ray crystallography

Molecular structures of complexes **2**, **3**, **5–8** which formed good quality crystals have been solved by X-ray Crystallography; the quality of other complexes was poor. The crystal of a complex was mounted on a polymer loop and data were measured on a Rigaku-Oxford Diffraction (**2**, **5–8**), Agilent, Eos, Gemini diffractometer (**3**) at 173(2) (**3**, **8**) and 293(2) (**2**, **5–7**) K. The diffractometer was equipped with a graphite monochromator with Mo–Kα radiation ($\lambda = 0.71073$ Å; **3**, **8**), or Cu-Kα radiation ($\lambda = 1.54178$ Å; **2**, **5–7**). The data collection and cell refinement were processed with CrysAlisPro while data reduction was processed with CrysAlisRED (**2**, **3**, **5–8**).[67] The structures were solved by the direct methods and refined using full-matrix least-squares techniques based on F^2 using ShelXL-2008, 2015.[68,69] Table 4 contains crystal data.

Antimicrobial studies

Test organisms and inoculum preparation. The reference strains of bacteria and yeast were obtained from Microbial Type Culture Collection (MTCC), Institute of Microbial Technology (IMTECH), Chandigarh, India. Reference strains included Gram positive bacteria: *Staphylococcus aureus* (MTCC 740), methicillin resistant *Staphylococcus aureus* (MRSA) *Staphylococcus epidermidis* (MTCC 435), *Enterococcus faecalis* (MTCC 439), Gram negative bacteria *Shigella flexneri* (MTCC 1457), *Escherichia coli* (MTCC 119) and a yeast *Candida albicans* (MTCC 227). A loopful of bacterial and yeast cells were inoculated into 5 mL of their respective broths and incubated at 37 °C and 25 °C, respectively for 4 h. This was used as inoculum after adjusting the turbidity as per the McFarland standard. This turbidity is equivalent to approximately (1 to 2) $\times 10^8$ colony forming units per mL (CFU per mL). The inoculums thus prepared were used for further testing.

Antimicrobial screening

A 100 μL of activated test organism (prepared as above) sample was inoculated onto suitable medium plates. Wells A 100 μL of activated test organism (prepared as above) sample was inoculated onto suitable medium plates by the spread plate method. Wells measuring 8 mm in diameter were cut out in the medium using a sterilized stainless steel borer. A stock solution of each test complex of concentration 50 mg mL^{-1} was prepared in DMSO and each well was filled with 0.1 mL of this test complex and kept for incubation in an upright position for 18–24 h. Sensitivity was measured in terms of a diameter of the zone of inhibition. Any organism with a clear zone of inhibition ≤12 mm was considered to be resistant to the compound.[70]

Minimum inhibitory concentration (MIC)

Minimum inhibitory concentration of the selected coordination compound dissolved in DMSO was worked out by the agar dilution method for their antimicrobial activity against the sensitive microorganisms. From the stock solution, the concentration of a complex in the range (0.001–2 mg mL^{-1}) was mixed with a Muller Hinton agar medium and then poured on plates. These plates were then inoculated with 0.1 mL of the activated bacterial and yeast strains by streaking with a sterile swab. The plates were incubated at 37 °C for bacteria and 25 °C for yeast for 24 h each. The minimum concentration of the extract causing inhibition of the visible growth was taken as MIC. The results were compared with that of DMSO as a control.

MTT toxicity assay

In order to check the level of cellular toxicity of the test compounds, MTT [3-(4,5-dimethylthiazol-2-yl)-2,5-diphenyl tetrazolium bromide] assay was performed[71] as follows. Ten milliliter of sheep blood was taken into an injection syringe containing 3 mL of Alsever's solution (anticoagulant) and transferred to sterile centrifuge tube. The blood was centrifuged at 16 000 rpm at room temperature (25 °C) for 20 min so as to separate the plasma from the cells. The supernatant was

discarded and 6 mL phosphate buffer saline (PBS) was added and it was again centrifuged. The blood cells were washed thrice with PBS by centrifugation and the pellet was re-suspended in 6 mL of PBS. Various dilutions of these cells were prepared using PBS and counted with the help of a hemocytometer under a light microscope so as to obtain cells equivalent to 1×10^5 cells per mL. One hundred microliters (100 μL) of this diluted suspension was added in each well and incubated at 37 °C for overnight. The supernatant was removed carefully and 200 μL of the sample solution (contains 10 mg mL^{-1}) was added and incubated further for 24 h. The supernatant was removed again and 20 μL MTT solution (5 mg mL^{-1}) was added to each well and incubated further for 3.5 h at 37 °C on an orbital shaker at 60 rpm. After incubation, the supernatant was removed without disturbing the cells and 50 μL of DMSO was added to each well to dissolve the formazan crystals. The absorbance was measured at 590 nm using an automated microplate reader (Biorad 680-XR, Japan). The wells with untreated cells served as a control. Reduction of MTT can only occur in metabolically active cells, as MTT is converted into formazan crystals and hence the absorbance directly represents the viability of the cells (% viability = (optical density (OD) of treated/OD of control) × 100). If the percent viability of the blood cells is quite high, then the compounds are non-cytotoxic in nature.

Antitumor studies

To determine *in vitro* cytotoxicity of silver(I) complexes of heterocyclic thiones, MTT assay MTT [3-(4,5-dimethylthiazol-2-yl)-2,5-diphenyl tetrazolium bromide],[72] was performed on a human osteosarcoma cell line, MG63. The cell line was procured from National Cell Center, Pune, India and was grown and matured in Dulbecco's Modified Eagle Medium (DMEM; Sigma-Aldrich) supplemented with 10% fetal bovine serum (FBS; Sigma-Aldrich) in tissue culture flask in the incubator supplied with 5% CO_2 at 37 °C and in 90% relative humidity provided by the growth medium. These cells were then collected in the confluent phase by treating with Trypsin-Hank's Balanced Salt Solution (HBSS). The cell suspension was centrifuged at 1500 rpm for 15 min. The supernatant was removed and 5 mL of medium (DMEM) was added to the cell pellet. The cell number was counted using hemocytometer under a light microscope and the cell density was made to 40 000 cell per mL (in DMEM) in the cell suspension.

The 100 μL of cell suspension was added to each well of the 96-well plate and the plate was kept in the CO_2 incubator with 5% CO_2, at 37 °C for 24 h. The culture was further incubated for 24 h in the presence of 100 μL of each of silver(I) complex of varying concentration (100, 50, 25, 12.5 and 6.25 μM) diluted in DMEM. The supernatant was removed from each well and 100 μL of MTT (0.5 mg mL^{-1} in DMEM) was added to each well, and further incubated at 37 °C for 4 h. After incubation, the supernatant was removed and the dark purple colored MTT formazan crystals were formed at the bottom of each of the well. The MTT formazan crystals thus formed were resuspended in 100 μL of dimethyl sulfoxide and the 96-well plate was shaken in a Labsystem Multiskan EX ELISA reader for 3 minute to dissolve the formazan crystals. The absorbance of the purple colored solution thus formed was then measured at 570 nm. The wells with untreated cells served as control. Reduction of MTT can only occur in metabolically active cells, as MTT is converted into formazan crystals and hence the absorbance directly represents the viability of the cells (% viability = (optical density (OD) of treated/OD of control) × 100). The IC_{50} values (50% inhibitory concentration), which is defined as the concentration of complex that reduced the number of living cancerous cells by 50%, were calculated from three independent experiments by generating an equation of logarithmic trend line of percentage cell viability against concentration of compounds in Microsoft excel.

Conflicts of interest

There are no conflicts to declare.

Acknowledgements

Financial assistance from the Council of Scientific and Industrial Research (CSIR), New Delhi for the Emeritus Scientist Grant [21(0904)/12-EMR-II] to T. S. L. is gratefully acknowledged. J. P. J. acknowledges the NSF-MRI program (Grant No. CHE-1039027) for funds to purchase the X-ray diffractometer.

References

1 S. Eckhardt, P. S. Brunetto, J. Gagnon, M. Priebe, B. Giese and K. M. Fromm, *Chem. Rev.*, 2013, **113**, 4708–4754.
2 K. M. Fromm, *Nat. Chem.*, 2011, **3**, 178.
3 P. S. Brunetto and K. M. Fromm, *Chimia*, 2008, **62**, 249–252.
4 G. McDonnell and A. D. Russell, *Clin. Microbiol. Rev.*, 1999, **12**, 147–179.
5 C. L. Fox and S. M. Modak, *Antimicrob. Agents Chemother.*, 1974, **5**(6), 582–588.
6 S. Bassetti, J. Hu, R. B. D'Agostino Jr and R. J. Sherertz, *Antimicrob. Agents Chemother.*, 2001, **45**, 1535–1538.
7 S. Shukla and A. P. Mishra, *J. Chem.*, 2013, 1–6.
8 A. T. Wan, R. A. J. Conyers, C. J Coombs and J. P. Masterton, *Clin. Chem.*, 1991, **37**, 1683–1687.
9 T. V. Slenters, I. Hauser-Gerspach, A. U. Daniels and K. M. Fromm, *J. Mater. Chem.*, 2008, **18**, 5359–5362.
10 P. G. Blower and J. R. Dilworth, *Coord. Chem. Rev.*, 1987, **76**, 121–185.
11 E. S. Raper, *Coord. Chem. Rev.*, 1994, **129**, 91–156.
12 E. S. Raper, *Coord. Chem. Rev.*, 1996, **153**, 199–255.
13 A. Sola, R. Lopez, A. Coxall and W. Clegg, *Eur. J. Inorg. Chem.*, 2004, 4871–4881.
14 T. S. Lobana, R. Sharma and R. J. Butcher, *Polyhedron*, 2008, **27**, 1375–1380.
15 G. A. Bowmaker, N. Chaichit, C. Pakawatchai, B. W. Skelton and A. H. White, *Can. J. Chem.*, 2009, **87**, 161–170.
16 A. Cingolani, F. Marchetti, C. Pettinari, R. Pettinari, B. W. Skelton and A. H. White, *Inorg. Chem.*, 2002, **41**, 1151–1161.

17 P. C. Zachariadis, S. K. Hadjikakou, N. Hadjiliadis, S. Skoulika, A. Michaelides, J. Balzarini and E. D. Clercq, *Eur. J. Inorg. Chem.*, 2004, 1420–1426.
18 L. Kyros, N. Kourkoumelis, M. Kubicki, L. Male, M. B. Hursthouse, I. I. Verginadis, E. Gouma, S. Karkabounas, K. Charalabopoulos and S. K. Hadjikakou, *Bioinorg. Chem. Appl.*, 2010, **2010**, 1–12.
19 J. S. Casas, E. G. Martinez, A. Sanchez, A. S. Gonzalez, J. Sordo, U. Casellato and R. Graziani, *Inorg. Chim. Acta*, 1996, **241**, 117–123.
20 P. Aslanidis, A. G. Hatzidimitriou, E. G. Andreadou, A. A. Pantazaki and N. Voulgarakis, *Mater. Sci. Eng., C*, 2015, **50**, 187–193.
21 P. Aslanidis, P. Karagiannidis, P. D. Akrivos, B. Krebs and M. Lage, *Inorg. Chim. Acta*, 1997, **254**, 277–284.
22 W. McFarlane, P. D. Akrivos, P. Aslanidis, P. Karagiannidis, C. Hatzisymeon, M. Numan and S. Kokkou, *Inorg. Chim. Acta*, 1998, **281**, 121–125.
23 P. A. Papanikolaou, A. G. Papadopoulos, E. G. Andreadou, A. Hatzidimitriou, P. J. Cox, A. A. Pantazakic and P. Aslanidis, *New J. Chem.*, 2015, **39**, 4830–4844.
24 G. A. Bowmaker, C. Pakawatchai, B. W. Skelton, Y. Thanyasirikul and A. H. White, *Z. Anorg. Allg. Chem.*, 2008, **634**, 2583–2588.
25 G. Giusti, G. Geier, A. Currao and R. Nesper, *Acta Crystallogr., Sect. C: Cryst. Struct. Commun.*, 1996, **52**, 1914–1917.
26 G. Christofidis, P. J. Cox and P. Aslanidis, *Polyhedron*, 2012, **31**, 502–505.
27 F. Jian, P. Sun, H. Xiao and K. Jiao, *Chin. J. Inorg. Chem.*, 2003, **9**, 979–982.
28 R. Sultana, T. S. Lobana, R. Sharma, A. castineiras, T. Akitsu, K. Yahagi and Y. Aritake, *Inorg. Chim. Acta*, 2010, **363**, 3432–3441.
29 P. Aslanidis, P. J. Cox, S. Divanidis and P. Karagiannidis, *Inorg. Chim. Acta*, 2004, **357**, 2677–2686.
30 S. Nawaz, A. A. Isab, K. Merz, V. Vasylyeva, N. Metzler-Nolte, M. Saleem and S. Ahmad, *Polyhedron*, 2011, **30**, 1502–1506.
31 P. Aslanidis, S. Divanidis, P. J. Cox and P. Karagiannidis, *Polyhedron*, 2005, **24**, 853–863.
32 P. A. Perez-Jourido, J. A. Garcia-Vazquez, J. Romero, M. S. Louro, A. Sousa, Q. Chen, Y. Chang and J. Zubieta, *J. Chem. Soc., Dalton Trans.*, 1996, 2047–2054.
33 W. Su, M. Hong, J. Weng, Y. Liang, Y. Zhao, R. Cao, Z. Zhou and A. S. C. Chan, *Inorg. Chim. Acta*, 2002, **331**, 8–15.
34 W. Su, R. Cao, M. Hong, W. T. Wong and J. Lu, *Inorg. Chem. Commun.*, 1999, **2**, 241–243.
35 S. I. Mostafa and N. Hadjiliadis, *Transition Met. Chem.*, 2008, **33**, 529–534.
36 S. K. Hadjikakou, I. I. Ozturk, M. N. Xanthopoulou, P. C. Zachariadis, S. Zartilas, S. Karkabounas and N. Hadjiliadis, *J. Inorg. Biochem.*, 2008, **102**, 1007–1015.
37 K. Nomiya, S. Takahashi and R. Noguchi, *J. Chem. Soc., Dalton Trans.*, 2000, 2091–2097.
38 S. A. Elsayed, B. J. Jean-Claude, I. S. Butler and S. I. Mostafa, *J. Mol. Struct.*, 2012, **1028**, 208–214.
39 N. R. F. M. Sofyan, F. J. Nordin, M. R. M. A. Razak, S. N. A. Halim, N. A. F. M. Khir, A. Muhammad, N. F. Rajab and R. Sarip, *J. Chem.*, 2018, **2018**, 1–10.
40 N. O. Al-Zamil, K. A. Al-Sadhan, A. A. Isab, M. I. M. Wazeer and A. R. A. Al-Arfaj, *Spectroscopy*, 2007, **21**, 61–67.
41 L. Kyros, C. N. Banti, N. Kourkoumelis, M. Kubicki, I. Sainis and S. K. Hadjikakou, *J. Biol. Inorg. Chem.*, 2014, **19**, 449–464.
42 I. Sainis, C. N. Banti, A. M. Owczarzak, L. Kyros, N. Kourkoumelis, M. Kubicki and S. K. Hadjikakou, *J. Inorg. Biochem.*, 2016, **160**, 114–124.
43 T. S. Lobana, R. Sultana, R. J. Butcher, J. P. Jasinski and T. Akitsu, *Z. Anorg. Allg. Chem.*, 2014, **640**, 1688–1695.
44 J. K. Aulakh, T. S. Lobana, H. Sood, D. S. Arora, V. A. Smolinski, C. E. Duff and J. P. Jasinski, *J. Inorg. Biochem.*, 2018, **178**, 18–31.
45 T. S. Lobana, R. Sultana and R. J. Butcher, *Dalton Trans.*, 2011, **40**, 11382–11384.
46 T. S. Lobana, R. Sultana, G. Hundal and R. J. Butcher, *Dalton Trans.*, 2010, **39**, 7870–7872.
47 T. S. Lobana, R. Sultana, R. J. Butcher, A. Castineiras, T. Akitsu, F. J. Fernandez and M. C. Vega, *Eur. J. Inorg. Chem.*, 2013, 5161–5170.
48 T. S Lobana and R. Sultana, *J. Chem. Sci.*, 2012, **124**, 1261–1268.
49 R. Sultana, T. S. Lobana and A. Castineiras, *RSC Adv.*, 2015, **5**, 100579–100588.
50 T. S. Lobana, R. Sultana, A. Castineiras and R. J. Butcher, *Inorg. Chim. Acta*, 2009, **362**, 5265–5270.
51 T. S. Lobana, R. Sultana, R. J. Butcher, J. P. Jasinski, J. A. Golen, A. Castineiras, K. Pröpper, F. J. Fernandez and M. C. Vega, *J. Organomet. Chem.*, 2013, **745–746**, 460–469.
52 T. S. Lobana, R. Sultana and G. Hundal, *Polyhedron*, 2008, **27**, 1008–1016.
53 T. S. lobana, R. Sultana, G. Hundal and A. Castineiras, *Polyhedron*, 2009, **28**, 1573–1577.
54 T. S. Lobana, R. Sharma, R. Sharma and R. J. Butcher, *Z. Anorg. Allg. Chem.*, 2008, **634**, 1785–1790.
55 T. S. Lobana, R. Sharma, E. Bermejo and A. Castineiras, *Inorg. Chem.*, 2003, **42**, 7728–7730.
56 T. S. Lobana, R. Sharma, G. Hundal and R. J. Butcher, *Inorg. Chem.*, 2006, **45**, 9402–9409.
57 T. S. Lobana, R. Sharma, R. Sharma, S. Mehra, A. Castineiras and P. Turner, *Inorg. Chem.*, 2005, **44**, 1914–1921.
58 J. K. Aulakh, T. S. Lobana, H. Sood, D. S. Arora, I. Garcia-Santos, G. Hundal, M. Kaur, V. A. Smolenski and J. P. Jasinski, *Dalton Trans.*, 2017, **46**, 1324–1339.
59 T. S. Lobana, J. K. Aulakh, H. Sood, D. S. Arora, I. Garcia-Santos, M. Kaur, C. E. Duff and J. P. Jasinski, *New J. Chem.*, 2018, **42**, 9886–9900.
60 B. Singh and K. P. Thakur, *J. Inorg. Nucl. Chem.*, 1974, **36**, 1735–1737.
61 J. E. Huheey, E. A. Keiter and R. L. Keiter, *Inorganic Chemistry: Principles of Structure and Reactivity*, Harper Collins, New York, 4th edn, 1993.
62 G. W. Anderson, I. F. Halverstadt, W. H. Miller and R. O. Roblin Jr, *J. Am. Chem. Soc.*, 1945, **67**, 2197–2200.

63 A. F. Eweas, Q. A. Abdallah and E. I. Hassan, *J. Appl. Pharm. Sci.*, 2014, **4**, 102–111.
64 C. S. W. Harker, E. R. T. Tiekink and M. W. Whitehouse, *Inorg. Chim. Acta*, 1991, **181**, 23–30.
65 J. A. Garcia-Vazquez, A. Sousa-Pedrares, M. Carabel, J. Romero and A. Sousa, *Polyhedron*, 2005, **24**, 2043–2054.
66 W. Walia, S. Kaur, J. Kaur, A. K. Sandhu, T. S. Lobana, G. Hundal and J. P. Jasinski, *Z. Anorg. Allg. Chem.*, 2015, **641**, 1728–1736.
67 Oxford Diffraction, *CrysAlisPro CCD and CrysAlisPro*, RED Oxford Diffraction Ltd., Abingdon, UK, 2010.
68 G. M. Sheldrick, *Acta Crystallogr., Sect. A: Found. Crystallogr.*, 2008, **64**, 112–122.
69 G. M. Sheldrick, *Acta Crystallogr., Sect. C: Cryst. Struct. Commun.*, 2015, **71**, 3–8.
70 D. S. Arora and J. Kaur, *Int. J. Antimicrob. Agents*, 1999, **12**, 257–262.
71 J. G. Onsare and D. S. Arora, *J. Appl. Microbiol.*, 2014, **118**, 313–325.
72 T. Mosmann, *J. Immunol. Methods*, 1983, **65**, 55–63.